

Discovery of the 2010 Eruption and the Pre-Eruption Light Curve for Recurrent Nova U Scorpii

Bradley E. Schaefer, Ashley Pagnotta, Limin Xiao

Physics and Astronomy, Louisiana State University, Baton Rouge, LA 70803

Matthew J. Darnley, Michael F. Bode

*Astrophysics Research Institute, Liverpool John Moores University, Birkenhead, CH41
1LD, UK*

Barbara G. Harris, Shawn Dvorak, John Menke, Michael Linnolt, Matthew Templeton,
Arne A. Henden

*American Association of Variable Star Observers, 49 Bay State Road, Cambridge MA
02138*

Grzegorz Pojmański, Bogumił Pilecki

Warsaw University Observatory, Al. Ujazdowskie 4, 00-478 Warszawa, Poland

Dorota M. Szczygiel,

*Department of Astronomy, The Ohio State University, 140 W. 18th Ave., Columbus OH
43210*

Yasunori Watanabe

*Variable Star Observers League of Japan, Keiichi Saijo National Science Museum,
Ueno-Park, Tokyo Japan*

ABSTRACT

We report the discovery by B. G. Harris and S. Dvorak on JD 2455224.9385 (2010 Jan 28.4385 UT) of the predicted eruption of the recurrent nova U Scorpii (U Sco). We also report on 815 magnitudes (and 16 useful limits) on the pre-eruption light curve in the UBVRI and Sloan r' and i' bands from 2000.4 up to 9 hours before the peak of the January 2010 eruption. We found no significant long-term variations, though we did find frequent fast variations (flickering) with amplitudes up to 0.4 mag. We show that U Sco did not have any rises or dips with amplitude greater than 0.2 mag on timescales from one day to one year before the eruption. We find that the peak of this eruption occurred at JD 2455224.69±0.07 and the start of the rise was at JD 2455224.32±0.12. From

our analysis of the average B-band flux between eruptions, we find that the total mass accreted between eruptions is consistent with being a constant, in agreement with a strong prediction of nova trigger theory. The date of the next eruption can be anticipated with an accuracy of ± 5 months by following the average B-band magnitudes for the next ~ 10 years, although at this time we can only predict that the next eruption will be in the year 2020 ± 2 .

Subject headings: novae, cataclysmic variables

1. Introduction

Recurrent novae (RNe) are ordinary novae (binary systems with mass accreting onto a white dwarf until thermonuclear runaway is triggered) for which the recurrence time scale is between a decade and a century, such that more than one eruption has been observed (Payne-Gaposchkin 1964; Bode & Evans 2008; Evans et al. 2008). To have the fast recurrence time scale, the novae must have the white dwarf near the Chandrasekhar mass and have a high accretion rate. These properties, at face value, imply that the white dwarf will soon exceed the Chandrasekhar mass and become a Type Ia supernova, and thus RNe are one of the premier candidates for the progenitor class of these supernovae. RNe typically have relatively fast eruptions, high ejection velocities, and small eruption amplitudes when compared to ordinary novae. Only ten RNe are known with certainty in our Milky Way (Schaefer 2010).

U Scorpii (U Sco) previously erupted in March 1999 with a peak at $V=7.5$ mag (Schaefer 2010). In quiescence, it has $V \approx 17.6$ and has deep *total* eclipses taking it down to $V=18.9$ mag (Schaefer 2010) with an orbital period of 1.23 days (Schaefer 1990; Schaefer & Ringwald 1995). U Sco is the fastest of all known novae, fading by three magnitudes from peak in just 2.6 days, while its rise from minimum to peak is 6-12 hours (Schaefer 2010). No light echo was detected to deep limits after the 1987 eruption (Schaefer 1988).

U Sco has now had ten known eruptions, in the years 1863, 1906, 1917, 1936, 1945, 1969, 1979, 1987, 1999 (Schaefer 2010), and now 2010 as we report in this paper. With the discovery of the 1917, 1945, and 1969 eruptions (Schaefer 2001; 2004), it has become apparent that U Sco has outbursts at intervals of 10 ± 2 years since 1900. The exceptions to this are the two intervals of 19 and 24 years, which are easily interpreted as being double intervals, with eruptions around 1927 and 1957 having been missed. (U Sco is 3.6° from the Sun every 28 November, so a significant fraction of its very fast eruptions must be missed.) With this, it became apparent that the next eruption of U Sco should occur in the year

2009 ± 2. Schaefer (2005) made a better prediction, on the physical basis that the time between eruptions scales as the inverse of the average mass accretion rate between eruptions (as measured from the B-band flux), with the scaling determined by the inter-eruption light curves from prior eruptions. The predicted eruption date was 2009.3 ± 1.0 . This is the first time that a specific star has been predicted to have an eruption on a specific date.

With this advance notice, a large international collaboration was formed to provide detailed photometry and spectroscopy in the X-ray, ultraviolet, optical, and infrared bands. With U Sco going from quiescence to peak to one magnitude below peak in 24 hours, we realized that we must have frequent monitoring of U Sco to get a fast alert of an eruption. To this end, we mobilized daily and hourly photometry with the SMARTS 1.3-m telescope in Chile, the fully-robotic 2.0-m Liverpool telescope (Steele et al. 2004) in the Canary Islands, and the four ROTSE 0.45-m telescopes in Australia, Texas, Namibia, and Turkey. In addition, we mobilized a large number of observers through the American Association of Variable Star Observers (AAVSO). For the seven months each year centered on the opposition of U Sco, we got hourly data. The headquarters of the AAVSO served as the international clearinghouse for discovery reports and delivery of alerts to the world. In addition, U Sco was heavily monitored from 2001 to 2009 with long time series photometry, where the main goal was to precisely measure the timing of the eclipses. The result of all this activity from 2000-2010 is the all-time best pre-eruption light curve for any nova. This paper presents all the magnitudes and an analysis of this large data set.

2. The Observations

Since 1987, one of us (BES) has heavily monitored U Sco, with emphasis on the light curve around the time of the eclipses (Schaefer 1990; 2005; 2010; Schaefer & Ringwald 1995). These observations have been made with the McDonald 2.7-m, 2.1-m, and 0.8-m telescopes in Texas as well as with the 1.3-m, 1.0-m, and 0.9-m telescopes on Cerro Tololo in Chile. The typical integration times were 300 seconds in the B-band and I-band and 100 seconds in the V-band. Normal processing was carried out, and the photometry was done using the IRAF package PHOT, which performs aperture photometry on the stars in this uncrowded field. The magnitude of U Sco was determined relative to a selection of nearby comparison stars, for which the primary comparison star, named ‘COMP’ (J2000 16:22:25.6 -17:51:34), has $B=16.96$, $V=15.87$, $R=15.25$, and $I=14.59$ (Schaefer 2010). The photon statistics, as calculated by PHOT, are generally smaller than 0.01 mag, but the systematic uncertainties, as represented by the scatter in the measures of standard star magnitudes (Landolt 1992; 2009), are typically 0.015 mag. The quoted uncertainty is the addition in quadrature of

0.015 mag and the uncertainty from photon statistics. This data set consists of over 2100 magnitudes, mostly as fast time series photometry centered on times of eclipses. The specific analysis of the eclipse shapes has already been presented in Schaefer (2010), while a specific analysis of the eclipse times is reserved for a separate paper. For the study in this paper, the eclipse effects would only hide the other variability, so we have not included any magnitudes with orbital phase between -0.10 and +0.10. In all, we have 162 magnitudes in the U, B, V, R, and I filters from 2001 to 2006.

Starting in early 2008, we (BES, AP, and LX) began frequent regular monitoring of U Sco with the 1.3-m SMARTS telescope on Cerro Tololo. This telescope is queue-scheduled, so an operator takes images of U Sco for us several times a week, thus allowing long-term frequent monitoring without requiring us to be at the telescope year-round. Most of the observations were 300 second exposures in the B-band, but we also made several sets of nearly simultaneous BVRI images. The procedures and analysis were identical to those described in the previous paragraph. In all, we have 145 magnitudes from early 2008 until late 2009.

Beginning in early 2008, one of us (BES) started using the robotic ROTSE telescopes to monitor U Sco once every hour. The ROTSE telescopes (Akerlof et al. 2003) are four automated 0.45-m f/1.9 telescopes with 1.85° fields designed to provide very fast response to satellite triggers on Gamma-Ray Bursts. The four telescopes are located at Coonabarabran, Australia; Mount Gamsberg, Namibia; Bakırtepe, Turkey; and McDonald Observatory, Texas. This wide coverage in longitude gives the potential for complete time coverage. No filters were used, so the resultant magnitudes are similar to a very broad R-band. The exposure time was 60 seconds in all cases. The requested cadence was one exposure every hour from every ROTSE telescope, but problems such as clouds, dawn, daylight, a nearby Full Moon, an altitude lower than 20° , higher priority alerts for Gamma-Ray Bursts, and the usual equipment problems all make for a substantially lower cadence. In the months around opposition, the ROTSE system achieved the ideal of nearly hourly coverage for around a quarter of the days, while the average coverage was roughly 15 images in every 24 hour interval. In the months approaching the conjunction of U Sco with the Sun, the daily coverage decreased to one or two images per 24 hour interval. For example, in 2009, ROTSE first recorded that U Sco was not in eruption on 9 January (43 days after conjunction) and last imaged U Sco on 18 October (40 days before conjunction). The limiting magnitude varied widely (with clouds, altitude, focus, and the Moon), yet U Sco was visible at low significance on about half the images. Even on the best images, U Sco did not get better than a 5-sigma detection, so in no case do we have accurate photometry from ROTSE. In all, we have a set of roughly 7000 useable U Sco images from ROTSE. One of the goals of the hourly monitoring by ROTSE was so that we (BES, AP, and MT) could frequently check

the images to try to discover the eruption as soon as possible. Another goal was to catch any pre-eruption rise (see Section 4) even if the amplitude was small and the duration was short. For the eruption in January 2010, there was no significant pre-eruption rise and our (BGH, SD, JM, ML) small-telescope monitoring produced a better light curve than ROTSE. A third reason for the ROTSE program was the hope that we would catch U Sco on the rise. In all previous eruptions, U Sco has been recorded on the rise only three times, each being close to the peak, with the rise from quiescence apparently lasting 6-12 hours (Schaefer 2010). In the hours before the discovery of the 2010 eruption, the Namibia ROTSE telescope did not look at U Sco due to a higher priority follow-up to a Gamma-Ray Burst, the Turkey ROTSE had clouds, and the Australia ROTSE was down with equipment problems. With the chance lack of any data on the rise and the poor photometric accuracy of the two years of monitoring, we are not presenting any of the ROTSE magnitudes in this paper.

Beginning in early 2008, we (MT and AAH) organized a steady watch on U Sco by the many observers of the AAVSO. The primary goal was to catch U Sco’s eruption as quickly as possible. The widespread distribution in longitude of the many AAVSO observers makes for frequent monitoring, and this was the best chance of catching the eruption early. For the half year around opposition, U Sco was checked for outburst up to 6.7 times per day for monthly averages. A further requirement for getting fast reactions from the world’s telescopes was that the discovery had to be communicated from the discoverer to the rest of the world. For this vital need, the AAVSO Headquarters served as an around-the-clock, every-day-of-the-year communication center. Observers were instructed to report their discovery electronically, then automated services would alert key individuals who would test for validity and solicit fast confirmation. Once the eruption was discovered, we would immediately start notifying the world through IAU Circulars and long-prepared phone and email lists.

As part of this effort, many AAVSO members made positive measures of the brightness of U Sco during the pre-eruption phase. The AAVSO database contains 412 magnitudes (from 29 observers) and 2853 limits (from 102 observers) between the end of the 1999 eruption and the start of the 2010 eruption (JD 2451557.148 to 2455224.127). The limits were vital at the time of the observation for knowing that U Sco had not erupted, but they are not now helpful for following the accretion rate. A further 77 magnitudes are not used here, primarily because the photometric system is not standard and the meaning of the magnitude would be unclear. This leaves us with 335 positive detections in the pre-eruption time interval. Just over 90% of these magnitudes were made with unfiltered CCD imaging, where the magnitudes were calibrated differentially from nearby comparison stars using either the V-band or R-band magnitudes. These magnitudes (designated CV or CR) will not be exactly on either the V or R magnitude systems, but the expected deviations (less than 0.1 mag) are always small compared to normal variations of U Sco. Our instrumentation is a 16-inch

f/10 Schmidt-Cassegrain with a V filter located in New Smyrna Beach, Florida (BGH), an 18-inch Newtonian telescope without filter located in Barnesville, Maryland (JM), and a 10-inch Schmidt-Cassegrain telescope with a V filter located in Clermont, Florida (SD). During the critical month before the eruption, all positive detections in the AAVSO database are provided by us (BGH and JM) from CCD images.

Beginning in early 2009, we (MJD and MFB) started monitoring U Sco with the robotic 2.0-m Liverpool Telescope (Steele et al. 2004) at the Observatorio del Roque de Los Muchachos on La Palma in the Canary Islands. The goals were to define the pre-eruption light curve in many bandpasses and perhaps to catch a pre-eruption rise or the eruption rise itself. The photometry was all differential with respect to the comparison stars given in Schaefer (2010). The images were usually taken through many filters in quick succession once each night. The filters we used were the B, V, Sloan r', and Sloan i'. Each light curve point consisted of three 60 s exposures. The data were analysed using Starlink software. The typical photometric errors had an uncertainty of 0.01-0.02 mag. In all, we present here 173 magnitudes from the Liverpool Telescope.

An important practical question was whether U Sco erupted during its yearly conjunction with the Sun every 28 November. The worst case scenario would be for U Sco to go up in early November, fade back to its quiescent level before any detection was made, and for the eruption to be completely missed. If U Sco went up while behind the Sun, it would be vital to know this so that our community would not be waiting anxiously with many resources, and also so that observations in the late tail could still be performed. For this, deep images would have to be made as far into twilight as possible. Professional telescopes do not go low enough in the sky, so the push into twilight was made entirely by AAVSO observers. For the November 2008 solar conjunction, U Sco was lost on 2 November and deep images showed U Sco to be near quiescence ($V > 16.1$) on 3 January, for a solar gap of 62 days. For the November 2009 solar conjunction, U Sco was last detected at $V = 18.6$ on 21 October (JM), was fainter than 12.0 mag on 4 November (ML), last checked on 6 November, while after conjunction our images showed it to be fainter than $V = 14.0$ on 27 December (ML), fainter than $V = 14.3$ on 28 December (ML), fainter than $V = 17.4$ on 30 December (BGH), and at quiescence ($V = 17.6$) on 4 January (BGH), for a solar gap of 51-59 days. From the V-band light curve template (Schaefer 2010; Schaefer et al. 2010b), U Sco is at $V = 16.6 \sim 42$ days after the peak. With this extremely short duration, the possibility for a missed eruption was for a peak from 3-23 November 2008 or 7-16 November 2009. As a chance to discover a U Sco eruption in the week around solar conjunction, one of us (SD) used the SOHO LASCO C3 instrument (which hides the Sun behind a white light coronagraph and produces images of stars, comets, and the corona out to 32 solar radii from the Sun) to demonstrate that the nova never came to peak (i.e., $V > 8.6$ mag) during that week-long interval.

The last positive detection of U Sco before its eruption was by us (BGH) on JD 2455223.9473. Nevertheless, there were later useful upper limits. Observing from the island of Hawaii, we (ML) used a 20-inch f/3.6 reflector to place a visual limit of >16.5 mag on JD 2455224.1271. The ASAS-3N telescope took a V-band image with a 180 second exposure on JD 2455224.1649 and we (GP, DMS, and BP) did not detect any source to a limit of 15.0 mag. This robotic telescope is located in Maui on Hawaii at an elevation of 3056 m, with a f/2.0 lens with focal length of 200 mm for a field of view of 8.5° on a side on a 2048x2048 pixel CCD chip. The last known observation before discovery (with $V > 9.2$) was taken by us (YW) on JD 2455224.3438 with a 60-mm f/5.9 refractor with an unfiltered CCD located in Yokosuka Japan.

From these sources, we have collected 815 magnitudes for U Sco between the end of the 1999 eruption and the discovery of the 2010 eruption. (We also report on 16 useful limits and the first three eruption magnitudes.) These are presented in Table 1. The first column lists the heliocentric Julian Date (HJD) of the observation. The second column gives the band of the observation. The third column gives the magnitude and the one-sigma uncertainty. The fourth column gives the source of the magnitude, either by identifying the telescope or by giving the AAVSO or VSOLJ observer identification code. HBB is for B. G. Harris, DKS is for S. Dvorak, MJLE is for J. Menke, LMK is for M. Linnolt, SCK is for B. E. Schaefer, and Wny is for Y. Watanabe. The next column is the orbital phase of U Sco (with primary eclipses at phase 0.0 and 1.0 and secondary eclipses at phase 0.5) for the pre-eruption ephemeris of $HJD = 2451234.539 + N \times 1.2305470$. The last column gives the fractional year corresponding to the Julian Date of the observation. Figure 1 displays the full light curve for the B filter, while Figure 2 shows the V band light curve after the start of 2009. Figure 3 shows the folded light curves for the B and V bands.

Table 2 lists various characteristic quantities (magnitudes, colors, and fluxes), their averages, their RMS scatters, and the number of observations going into the averages. For the science of this paper, we are only interested in the non-eclipsing behavior, so to be conservative, we have included only measures more than 0.10 in phase (0.123 in days) away from the central eclipse times (i.e., between phases 0.10 and 0.90). For the colors, we have included only those colors derived from two magnitudes taken within 0.005 days of each other so as to keep the errors introduced by fast variations to a minimum. The overall magnitudes (for all bands) and colors for the entire time interval (from 2000 to the 2010 eruption) are recorded. We also break up the B and V band magnitudes into smaller intervals so as to seek significant variations. Finally, we include the average B-band fluxes as defined in Section 6.

3. Discovery of the 2010 Eruption

The 2010 Eruption was discovered by us (BGH and SD) as part of systematic nightly monitoring aimed specifically at the discovery of the eruption. Harris imaged U Sco at 2010 Jan 28.4385 UT (JD 2455224.9385), saw the bright star in the center of the field, and quickly realized that U Sco was in eruption. Her first act was to send the observation to the AAVSO, and then she telephoned Schaefer. Schaefer could not get confirmation from ROTSE, so he took his 6-inch telescope out into the front yard and made direct visual confirmation that U Sco was bright in eruption. Independently, Dvorak discovered the eruption, notified the AAVSO, and started a time series on U Sco to cover the short time interval until dawn got too bright to continue. These initial observations are included in Table 1. Circumstances, pictures, and anecdotes on the two independent discoveries are given in Simonsen & MacRobert (2010).

In practice, our organization worked perfectly. The AAVSO automated alert system woke up MT and AP. Within an hour of the discovery, the eruption had been confirmed and worldwide notifications were started. The first was to the IAU Circulars (Schaefer et al. 2010a). The sun had already risen in Chile, so we started with more western observatories as well as spacecraft. Within two hours, BES, AP, and MT had worked through all the long-prepared contact lists. The response to these contacts (both by members of our existing collaboration as well as by independent observers) was excellent and fast.

The discovery of the 2010 eruption was a fulfillment of the prediction in Schaefer (2005) that U Sco would next erupt in the year 2009.3 ± 1.0 . The eruption in 2010.1 falls well within the one-sigma region of the prediction. This adds good confidence to the physical method of summing the total accreted material based on the B-band flux in the prior inter-eruption interval.

4. Variations in the Light Curve

The folded light curve (see Figure 3) shows the primary eclipse at phases 0.0, 1.0, and 2.0. (The magnitudes are double plotted so as to make the eclipse at phase 1.0 easily visible.) The out-of-eclipse brightness varies substantially, and this makes for a ragged eclipse light curve because each point is from a different epoch eclipse with a different amount of flickering light added. The scatter around the middle of the eclipse is much smaller than the out-of-eclipse scatter, which implies that the flickering region is small and centrally located.

No secondary eclipse is visible in the B and V bands. However, in the I-band, the secondary eclipse is visible with amplitude roughly 0.3 mag. This is readily understood as

the companion star is much cooler than the accretion disk so eclipses of the companion can only become noticeable at longer wavelength.

All cataclysmic variables, including novae and recurrent novae, show fast flickering. U Sco is no exception, and this flickering causes the substantial scatter in Figures 1 and 2. To quantify this, we have calculated the magnitude difference between pairs of magnitudes in the same band, with the pairs being separated in time by some range of delays. When the delays are shorter than one hour, the RMS scatter of the magnitude differences is 0.06 mag, which is consistent with the expected scatter as based only on the quoted error bars. When the delays are longer than one day, the RMS scatter of the magnitude differences is 0.27, which corresponds to no correlation between the flickers. The RMS scatters are 0.09, 0.13, 0.18, 0.19, and 0.21 mag for delays of 0.05-0.10, 0.10-0.15, 0.15-0.20, 0.20-0.50, and 0.50-1.00 days, respectively. With this, the timescale for correlated variations is from one hour to one day. The amplitude of these variations is given by the maximum values of the magnitude differences, which is roughly 0.4 mag for all delays longer than 0.05 days. Our observations are not sensitive to fast, small-amplitude variations.

Many of the recurrent novae have large secular variations in their quiescent light curves (Schaefer 2010). However, U Sco does not appear to have any long-term variations, as can be seen in Figure 1. To quantify this for the B and V light curves, Table 2 gives the averages for various time intervals. Again, no significant variations on time scales of one year or longer are found, despite having small error bars due to the many magnitudes included in the averages. On the timescale of a tenth of a year, there is marginal evidence for variations, with the V-band average for 2009.7-2009.9 being 0.27 ± 0.05 fainter than average, but this variation is not reflected in other bands, so we think that this apparent change is not significant. In all, we see no evidence for variations on timescales from 0.1 to 10 years.

On longer times scales, U Sco has small, marginally-significant variations. During the last four inter-eruption intervals, the average B magnitude was 18.44 ± 0.07 , 18.30 ± 0.05 , and 18.52 ± 0.04 , and 18.45 ± 0.02 for 1969-1979, 1979-1987, 1987-1999 (Schaefer 2005), and 1999-2010 respectively. The chi-square for the observed averages (on the hypothesis that the average is a constant) is 12.1 for three degrees of freedom. The best argument for the significance of these variations is that the deviations from the average are correlated with the duration of each inter-eruption time interval as predicted by theory (see Section 7).

The earliest recorded image of U Sco in quiescence is from the original Palomar Sky Survey. We measure $B=18.80 \pm 0.15$ and $R=18.00 \pm 0.18$ for 29 June 1954. This is substantially fainter than is normal for later decades, and the time is far from any plausible eclipse.

5. No Pre-eruption Rise or Dip

Robinson (1975) examined all known pre-eruption light curves of novae as based on reports in the literature. He found that five out of eleven novae have pre-eruption rises, lasting months to years in advance of the eruption, with amplitudes from 0.15 to 1.5 mag. Collazzi et al. (2009) have gone to the original archival photographic plates to measure many pre-eruption light curves, including the key novae with claimed pre-eruption rises. Four of the five claimed pre-eruption rises were found not to exist as based on our examination of the original plates, such that the claimed rises were caused by simple errors in the literature. Nevertheless, one of the rises (for V533 Her) was confirmed and extended, with the rise being an exponential increase over \sim 1.5 years and a brightening by up to 1.5 mag. Also, an additional pre-eruption rise was confirmed in V1500 Cyg, which brightened from roughly 21.5 mag to roughly 13 mag in the month preceding the eruption. (V1500 Cyg had the fastest known *classical* nova eruption, and was second only to U Sco itself amongst all novae.) In addition, a complex pre-eruption dip was confirmed for the recurrent nova T CrB in the year before the eruption, with the dip being 1-2 mag deep. In all, three out of 22 novae had either pre-eruption rises or pre-eruption dips.

With other recurrent novae and the fastest classical nova having anticipatory rises and dips, we should investigate whether U Sco has any similar changes. (We were also hopeful that any such phenomenon would allow us to anticipate the next eruption.) For this, we can use our light curves to seek any rises or dips. A glance at Figure 1 quickly shows that there is no significant rise or dip. Quantitatively, Table 2 shows that the B and V magnitudes from 2010.0-2010.1 are not significantly high or low. And looking at the bottom of Table 1, we see that the last positive detection of U Sco has $V=18.2$ (BGH) just 24 hours before the discovery. With this, we can put strong limits on the presence of any pre-eruption rise or dip to be less than roughly 0.2 mag in amplitude on time scales from one day up to a year.

6. The Rise to Peak

U Sco rises from quiescence to peak in roughly 6-12 hours, although this is based on just three pre-peak positive detections and one limit (Schaefer 2010). For the 1936 eruption, a single Harvard plate shows $B=10.75$ at a time 0.25 days before peak. For the 1987 eruption, Dr. N. W. Taylor measured $V=14.0$ in the day before the peak. For the 1999 eruption, P. Schmeer measured $V=9.5$ at a time 0.31 days before the peak. The final rise to maximum is at a rate of around 19 magnitudes per day, which would imply a rise time of roughly 12 hours if the rise is uniform throughout. For the 1999 eruption, B. Monard set a limit that $V > 14.3$ at a time 0.46 days before the peak.

We can use our data to obtain the best estimate for the time of peak in the 2010 eruption. The discovery image was taken at JD 2455224.9385 (BGH), and we have measured the magnitude of U Sco (with respect to the comparison star sequence in Schaefer 2010) to be V=7.85 with the systematic uncertainties dominating at around 0.10 mag. The observed initial rate of decline is 1.4 mag per day (Schaefer et al. 2010b). The peak magnitude of U Sco is V=7.5, primarily as based on the observed peak of the 1999 eruption (Schaefer 2010). In an exhaustive comparison of all RN eruptions and those from U Sco in particular, Schaefer (2010) found that all RN are consistent with having the identical eruption light curve shapes, and this is our basis for taking the peak from the 1999 U Sco eruption as being the same for the 2010 eruption. With this, the peak of the 2010 eruption would have been 0.25 days before discovery, which gives a peak at JD 2455224.69 with a likely uncertainty of 0.07 days.

The observational limits from the 2010 eruption show that the eruption could not have started much before the ASAS-3N image at JD 2455224.1649. From the limits on the prior eruptions, the eruption started 0.25 to 0.5 days before the peak, which is roughly from JD 2455224.19 to 2455224.44. Thus, the time of the start of the expansion, as required by the ‘universal decline law’ of Hachisu & Kato (2006), can be expressed as JD 2455224.32±0.12.

Disappointingly, we have no observations from JD 2455224.3438 to 2455224.9385 and thus have completely missed the entire rise and the hour of peak. In January, U Sco is fairly close to the Sun and hence only visible from a narrow slice of longitude at any given time. In the southern hemisphere, the start of the rise would only have been visible from the longitudes in the Indian Ocean, while the peak would only have been visible from the longitudes in the South Atlantic Ocean.

7. Predicting the Next Eruption

Schaefer (2005) presented a new method for predicting the date of the next eruption of a recurrent nova based on the requirement that some constant amount of mass must be accumulated by the white dwarf between eruptions. Accretion rates vary substantially (Schaefer 2010; and see Figure 1), so the interval between eruptions (T) depends on the average accretion during that time. If the accretion rate is high then the interval will be short, while if the accretion rate is low then T will be high. For U Sco, the blue light is dominated by the accretion disk, so the blue flux (F_B) will be a measure of the accretion rate. In particular for U Sco, the accretion rate will be proportional to $F_B^{1.5}$ (Schaefer 2005). By averaging $F_B^{1.5}$ over each interval T , we can derive a quantity that is proportional to the average accretion rate. Then, $\langle F_B^{1.5} \rangle T$ should be proportional to the total mass accreted

between eruptions, which should be a constant. Schaefer (2005) found that this quantity is indeed constant for four intervals for T Pyx and three intervals for U Sco (despite widely varying values of T for each system), with this providing a good test of nova trigger theory. These *observed* values for $\langle F_B^{1.5} \rangle T$ provide empirical measures of the mass required to trigger the eruptions. Then, based on the observed B magnitudes up until 2005, Schaefer (2005) was able to predict that U Sco would next erupt in 2009.3 ± 1.0 . Schaefer (2010) updated the situation to arrive at the same predicted date. As noted above, the actual eruption on 2010.1 falls well within this prediction.

Now, with the full pre-eruption light curve, we can better test the prediction and we can refine the constant for use in predicting the next eruption. To this end, we have first converted the B-band magnitudes to flux units where B=18 is taken to be the unit flux ($F_{B,18}$), which equals $10^{(18-B)/2.5}$. The accretion rate will then be proportional to $F_{B,18}^{1.5}$. To get the time averaged value from 2000-2010.1, we should not simply average all the values, as this would produce a high weight to the behavior of U Sco during 2008 and 2009 (during which the majority of the B-band magnitudes were taken). Instead, we have taken time intervals and combined them with weights given by their duration. In Table 2, we list the average values of the measured $F_{B,18}^{1.5}$ for three intervals with roughly constant frequency of observations. The uncertainty in these averages is the RMS scatter divided by the square root of the number of observations. The durations of these intervals were then used as weights for averaging the intervals, and the uncertainty in the overall average comes from the usual propagation of errors. The resultant average over the entire interval between the 1999.2 and 2010.1 eruption is listed in Table 2. In all, $\langle F_{B,18}^{1.5} \rangle = 0.577 \pm 0.045$.

Schaefer (2005) produces values of $\langle F_B^{1.5} \rangle$ for the three prior inter-eruption intervals. These need to be updated for four reasons. First, we need to standardize to the same flux level (i.e., B=18) as the unit flux. Second, we should be consistent and not include any magnitudes within phase 0.10 of the eclipse. Third, the individual observations should be formed into the averages with equal weight (instead of weighted by the measurement uncertainty) because intrinsic fluctuations are substantially larger than the measurement errors (so we would not want to give high weight to a bright point simply because it has a small error bar). Fourth, the 1969-1979 interval has only two magnitudes, so instead of determining the uncertainty based on the RMS scatter of just these two, we have equated the scatter to that during the 1987-1999 interval. The resultant $\langle F_{B,18}^{1.5} \rangle$ values are given in Table 2.

U Sco erupted in the years 1969, 1979, 1987, 1999, and 2010, with T values of 10.4, 7.9, 11.8, and 10.9 years for the four inter-eruption intervals. The longest interval is a factor of $1.5 \times$ the shortest interval. We see that the shortest interval has the highest average

accretion rate, while the longest interval has the lowest average accretion rate, and the two middle intervals have the middle average accretion rates. The four intervals in time order have $\langle F_{B,18}^{1.5} \rangle T$ values of 5.7 ± 1.2 , 5.2 ± 0.4 , 6.0 ± 0.4 , and 6.3 ± 0.5 . (The weighted average of these four values is 5.77 ± 0.24 .) Nova trigger theory predicts that these values should be a constant. Indeed, the chi-square equals 3.4 for the hypothesis that the four values are equal to a constant, which is acceptable given the three degrees of freedom. And we see that the values are consistent with being a constant despite T varying by up to a factor of 1.5. So we have an improved confirmation of nova trigger theory.

U Sco erupted in 1945 and 1969, with an inter-eruption interval of 23.7 years. The long interval could be because *one* eruption was missed around 1957 (with intervals of around 11.8 and 11.9 years) or because *two* eruptions were missed around 1953 and 1961 (with intervals of around 7.9, 7.9, and 7.9 years). These two possibilities can be distinguished due their greatly different prediction as to the quiescent B magnitude, roughly 18.52 versus 18.30 respectively. The one measured magnitude ($B=18.80 \pm 0.15$ from 1954.5) suggests that the accretion rate was low, and hence that there was only one missed eruption.

When will the next eruption of U Sco occur? Over the next decade, we can keep track of the B-band magnitudes and work out when $\langle F_{B,18}^{1.5} \rangle T$ will equal 5.77 ± 0.24 . Such a prediction will only be accurate to roughly 5 months out of ten years, which is fairly good. However, this method cannot be used yet, because we cannot predict the variations in the U Sco accretion rate. For now, the best that we can do is to use the long record of U Sco where all of its inter-eruption intervals are 10 ± 2 years. With this, we predict the next U Sco eruption to be in 2020 ± 2 .

We thank the many observers from the American Association of Variable Stars Observers for their data as used in our light curves. This work is supported under a grant from the National Science Foundation (AST 0708079). The Liverpool Telescope is operated on the island of La Palma by Liverpool John Moores University in the Spanish Observatorio del Roque de los Muchachos of the Instituto de Astrofísica de Canarias with financial support from the UK Science and Technology Facilities Council.

REFERENCES

- Akerlof, C. W. et al. 2003, PASP, 115, 132
Bode, M. F. & Evans, A. 2008, Classical Novae, 2nd edition (Cambridge, Cambridge Univ. Press)

- Collazzi, A.C., Schaefer, B.E., Xiao, L., Pagnotta, A., Kroll, P., Löchel, K. & Henden, A.A. 2009, AJ, 138, 1846
- Evans, A., Bode, M. F., O'Brien, T. J. & Darnley, M. J. 2008, RS Ophiuci (2006) and the Recurrent Nova Phenomenon (ASP Conf. 401)
- Hachisu, I. & Kato, M. 2006, ApJSupp, 167, 59
- Landolt, A. U. 1992, AJ, 104, 340
- Landolt, A. U. 2009, AJ, 137, 4186
- Payne-Gaposkin, C. 1964, The Galactic Novae (Dover, New York)
- Robinson, E. L. 1975, AJ, 80, 515
- Schaefer, B. E. 1988, ApJ, 327, 347
- Schaefer, B. E. 1990, ApJLett, 355, L39
- Schaefer, B. E. 2001, IAUCirc., 7749
- Schaefer, B. E. 2004, IAUCirc., 8279
- Schaefer, B. E. 2005, ApJLett, 621, L53
- Schaefer, B. E. 2010, ApJSupp, 187, 275
- Schaefer, B. E., Harris, B. G., Dvorak, S., & Linnolt, M. 2010a, IAUCirc., 9111
- Schaefer, B. E. & Ringwald, F. A. 1995, ApJLett, 447, L45
- Schaefer, B. E. et al. 2010b, ATel, 2507
- Simonsen, M. & MacRobert, A. 2010, Sky & Telescope, 119, No. 5, 18
- Steele, I. A. et al. 2004, Proc. SPIE, 5489, 679

Table 1. U Sco Pre-eruption Light Curve

HJD	Band	Magnitude	Source	Phase	Year
2451702.1932	CV	18.1 ± 0.1	AAVSO (LAQ)	0.038	2000.432
2451708.1195	CV	18.6 ± 0.1	AAVSO (LAQ)	0.854	2000.448
2451719.0413	CV	18.8 ± 0.1	AAVSO (LAQ)	0.729	2000.478
2452016.8446	V	17.90 ± 0.01	McDonald 2.1m	0.738	2001.293
2452018.8356	V	18.05 ± 0.02	McDonald 2.1m	0.356	2001.299
2452018.8397	R	17.69 ± 0.01	McDonald 2.1m	0.359	2001.299
2452021.7832	R	17.61 ± 0.02	McDonald 2.1m	0.751	2001.307
2452021.7864	R	17.63 ± 0.01	McDonald 2.1m	0.754	2001.307
2452021.7895	R	17.61 ± 0.02	McDonald 2.1m	0.757	2001.307
2452021.7925	R	17.54 ± 0.02	McDonald 2.1m	0.759	2001.307
2452021.7956	R	17.57 ± 0.01	McDonald 2.1m	0.761	2001.307
2452021.7986	R	17.58 ± 0.01	McDonald 2.1m	0.764	2001.307
2452021.8588	R	17.47 ± 0.01	McDonald 2.1m	0.813	2001.307
2452021.8621	V	17.84 ± 0.01	McDonald 2.1m	0.816	2001.307
2452021.9508	R	17.52 ± 0.01	McDonald 2.1m	0.888	2001.307
2452022.8163	R	17.34 ± 0.01	McDonald 2.1m	0.591	2001.310
2452022.8197	V	17.67 ± 0.01	McDonald 2.1m	0.594	2001.310
2452022.9468	V	17.74 ± 0.02	McDonald 2.1m	0.697	2001.310
2452022.9506	R	17.34 ± 0.01	McDonald 2.1m	0.700	2001.310
2452125.6972	V	17.98 ± 0.04	McDonald 2.1m	0.197	2001.591
2452125.7101	I	17.24 ± 0.03	McDonald 2.1m	0.207	2001.591
2452125.7118	V	18.24 ± 0.05	McDonald 2.1m	0.209	2001.591
2452127.6580	V	17.99 ± 0.02	McDonald 2.1m	0.790	2001.597
2452127.6594	I	17.16 ± 0.01	McDonald 2.1m	0.791	2001.597
2452127.6616	I	17.15 ± 0.02	McDonald 2.1m	0.793	2001.597
2452127.6686	V	18.00 ± 0.03	McDonald 2.1m	0.799	2001.597
2452130.6395	V	18.06 ± 0.01	McDonald 2.1m	0.213	2001.605
2452130.6480	B	18.33 ± 0.02	McDonald 2.1m	0.220	2001.605
2452426.8409	B	18.86 ± 0.02	McDonald 2.1m	0.920	2002.416
2452426.8452	B	18.83 ± 0.03	McDonald 2.1m	0.924	2002.416
2452426.8497	B	18.92 ± 0.03	McDonald 2.1m	0.927	2002.416
2452426.8537	V	18.35 ± 0.02	McDonald 2.1m	0.931	2002.416
2452426.8587	V	18.17 ± 0.02	McDonald 2.1m	0.935	2002.416
2452426.8624	V	18.38 ± 0.03	McDonald 2.1m	0.938	2002.416
2452431.6794	B	18.17 ± 0.01	McDonald 2.1m	0.852	2002.429
2452431.6834	B	18.15 ± 0.01	McDonald 2.1m	0.856	2002.429
2452431.6863	I	17.34 ± 0.01	McDonald 2.1m	0.858	2002.429
2452431.6879	I	17.36 ± 0.02	McDonald 2.1m	0.859	2002.429
2452761.5052	CR	17.9 ± 0.1	AAVSO (MLF)	0.884	2003.332
2452763.4203	CR	17.7 ± 0.1	AAVSO (MLF)	0.440	2003.337
2452765.8658	I	17.61 ± 0.02	McDonald 0.8m	0.428	2003.344
2452765.8724	B	19.03 ± 0.04	McDonald 0.8m	0.433	2003.344
2452769.7860	I	17.36 ± 0.02	McDonald 0.8m	0.613	2003.355
2452769.7926	B	18.73 ± 0.04	McDonald 0.8m	0.619	2003.355
2452786.7196	I	16.61 ± 0.02	McDonald 0.8m	0.375	2003.401
2452786.7243	V	18.13 ± 0.03	McDonald 0.8m	0.378	2003.401

Table 1—Continued

HJD	Band	Magnitude	Source	Phase	Year
2452891.2341	CR	17.3 ± 0.1	AAVSO (MLF)	0.308	2003.687
2453054.5003	CR	17.5 ± 0.1	AAVSO (MLF)	0.986	2004.134
2453054.6003	CR	17.5 ± 0.1	AAVSO (MLF)	0.067	2004.134
2453068.5397	V	17.5 ± 0.1	AAVSO (MLF)	0.395	2004.173
2453082.9035	U	19.03 ± 0.06	McDonald 0.8m	0.067	2004.212
2453082.9111	B	19.30 ± 0.04	McDonald 0.8m	0.074	2004.212
2453082.9153	V	18.65 ± 0.03	McDonald 0.8m	0.077	2004.212
2453082.9247	R	18.18 ± 0.03	McDonald 0.8m	0.085	2004.212
2453082.9288	I	17.59 ± 0.04	McDonald 0.8m	0.088	2004.212
2453092.5279	CR	17.2 ± 0.1	AAVSO (MLF)	0.889	2004.238
2453130.3553	CR	17.8 ± 0.1	AAVSO (MLF)	0.629	2004.342
2453136.6145	CR	17.5 ± 0.1	AAVSO (MLF)	0.715	2004.359
2453152.4188	CR	17.7 ± 0.1	AAVSO (MLF)	0.559	2004.402
2453171.2315	CR	17.6 ± 0.1	AAVSO (MLF)	0.847	2004.454
2453172.2325	CR	17.5 ± 0.1	AAVSO (MLF)	0.660	2004.456
2453182.2841	CR	17.4 ± 0.1	AAVSO (MLF)	0.829	2004.484
2453187.7869	V	18.16 ± 0.16	CTIO 1.0m	0.301	2004.499
2453187.7885	V	18.27 ± 0.07	CTIO 1.0m	0.302	2004.499
2453187.7934	R	17.99 ± 0.05	CTIO 1.0m	0.306	2004.499
2453187.7979	I	17.36 ± 0.06	CTIO 1.0m	0.309	2004.499
2453187.8024	I	17.43 ± 0.05	CTIO 1.0m	0.313	2004.499
2453187.8104	B	18.29 ± 0.11	CTIO 1.0m	0.320	2004.499
2453189.4895	R	17.98 ± 0.06	CTIO 1.0m	0.684	2004.504
2453189.4911	B	18.58 ± 0.07	CTIO 1.0m	0.685	2004.504
2453189.4988	B	18.67 ± 0.05	CTIO 1.0m	0.692	2004.504
2453189.5065	V	18.33 ± 0.03	CTIO 1.0m	0.698	2004.504
2453189.5144	R	17.91 ± 0.02	CTIO 1.0m	0.704	2004.504
2453189.5225	I	17.43 ± 0.02	CTIO 1.0m	0.711	2004.504
2453189.5733	I	17.48 ± 0.08	CTIO 1.0m	0.752	2004.504
2453189.5741	I	17.46 ± 0.03	CTIO 1.0m	0.753	2004.504
2453189.5814	I	17.47 ± 0.02	CTIO 1.0m	0.759	2004.504
2453189.6682	I	17.39 ± 0.07	CTIO 1.0m	0.829	2004.504
2453189.6705	I	17.41 ± 0.02	CTIO 1.0m	0.831	2004.504
2453189.6781	I	17.42 ± 0.02	CTIO 1.0m	0.837	2004.504
2453191.4873	I	17.39 ± 0.02	CTIO 1.0m	0.308	2004.509
2453191.4948	I	17.47 ± 0.03	CTIO 1.0m	0.314	2004.509
2453191.5191	I	17.41 ± 0.03	CTIO 1.0m	0.333	2004.509
2453191.5265	I	17.36 ± 0.02	CTIO 1.0m	0.339	2004.509
2453191.5443	I	17.42 ± 0.03	CTIO 1.0m	0.354	2004.509
2453191.5521	I	17.40 ± 0.02	CTIO 1.0m	0.360	2004.509
2453191.5761	I	17.44 ± 0.03	CTIO 1.0m	0.380	2004.509
2453191.5836	I	17.44 ± 0.03	CTIO 1.0m	0.386	2004.509
2453191.6033	I	17.56 ± 0.04	CTIO 1.0m	0.402	2004.510
2453191.6105	I	17.50 ± 0.03	CTIO 1.0m	0.408	2004.510
2453191.6607	I	17.51 ± 0.03	CTIO 1.0m	0.449	2004.510
2453191.6696	I	17.54 ± 0.03	CTIO 1.0m	0.456	2004.510

Table 1—Continued

HJD	Band	Magnitude	Source	Phase	Year
2453191.6923	I	17.46 ± 0.03	CTIO 1.0m	0.474	2004.510
2453191.6995	I	17.49 ± 0.03	CTIO 1.0m	0.480	2004.510
2453191.7078	I	17.52 ± 0.03	CTIO 1.0m	0.487	2004.510
2453191.7153	I	17.56 ± 0.03	CTIO 1.0m	0.493	2004.510
2453191.7225	I	17.53 ± 0.03	CTIO 1.0m	0.499	2004.510
2453191.7300	I	17.54 ± 0.04	CTIO 1.0m	0.505	2004.510
2453191.7373	I	17.55 ± 0.04	CTIO 1.0m	0.511	2004.510
2453191.7448	I	17.54 ± 0.04	CTIO 1.0m	0.517	2004.510
2453191.7520	I	17.54 ± 0.04	CTIO 1.0m	0.523	2004.510
2453191.7594	I	17.42 ± 0.04	CTIO 1.0m	0.529	2004.510
2453191.7667	I	17.47 ± 0.04	CTIO 1.0m	0.535	2004.510
2453191.7743	I	17.46 ± 0.04	CTIO 1.0m	0.541	2004.510
2453191.7816	I	17.47 ± 0.05	CTIO 1.0m	0.547	2004.510
2453192.5670	I	17.30 ± 0.03	CTIO 1.0m	0.185	2004.512
2453194.6257	I	17.31 ± 0.03	CTIO 1.0m	0.858	2004.518
2453194.6311	I	17.36 ± 0.03	CTIO 1.0m	0.862	2004.518
2453195.4959	I	17.31 ± 0.02	CTIO 1.0m	0.565	2004.520
2453195.4984	I	17.33 ± 0.02	CTIO 1.0m	0.567	2004.520
2453195.5132	I	17.33 ± 0.02	CTIO 1.0m	0.579	2004.520
2453195.5204	I	17.34 ± 0.02	CTIO 1.0m	0.585	2004.520
2453195.5277	I	17.30 ± 0.02	CTIO 1.0m	0.591	2004.520
2453195.5350	I	17.29 ± 0.02	CTIO 1.0m	0.597	2004.520
2453195.5424	I	17.27 ± 0.02	CTIO 1.0m	0.603	2004.520
2453195.5496	I	17.25 ± 0.02	CTIO 1.0m	0.609	2004.520
2453195.5569	I	17.25 ± 0.02	CTIO 1.0m	0.615	2004.520
2453195.5642	I	17.26 ± 0.02	CTIO 1.0m	0.621	2004.520
2453195.5716	I	17.25 ± 0.02	CTIO 1.0m	0.627	2004.520
2453195.5788	I	17.28 ± 0.02	CTIO 1.0m	0.633	2004.520
2453195.5861	I	17.30 ± 0.02	CTIO 1.0m	0.639	2004.520
2453195.5934	I	17.28 ± 0.02	CTIO 1.0m	0.644	2004.520
2453195.6007	I	17.29 ± 0.02	CTIO 1.0m	0.650	2004.520
2453195.6080	I	17.31 ± 0.02	CTIO 1.0m	0.656	2004.520
2453195.6171	I	17.28 ± 0.02	CTIO 1.0m	0.664	2004.521
2453195.6244	I	17.25 ± 0.02	CTIO 1.0m	0.670	2004.521
2453195.6316	I	17.21 ± 0.02	CTIO 1.0m	0.676	2004.521
2453195.6389	I	17.23 ± 0.02	CTIO 1.0m	0.681	2004.521
2453195.6463	I	17.24 ± 0.02	CTIO 1.0m	0.687	2004.521
2453195.6536	I	17.23 ± 0.02	CTIO 1.0m	0.693	2004.521
2453195.6609	I	17.23 ± 0.02	CTIO 1.0m	0.699	2004.521
2453196.4771	I	17.23 ± 0.02	CTIO 1.0m	0.363	2004.523
2453196.4920	I	17.24 ± 0.02	CTIO 1.0m	0.375	2004.523
2453196.4993	I	17.27 ± 0.02	CTIO 1.0m	0.381	2004.523
2453196.5065	I	17.28 ± 0.02	CTIO 1.0m	0.386	2004.523
2453196.5141	I	17.29 ± 0.02	CTIO 1.0m	0.393	2004.523
2453196.5274	I	17.31 ± 0.02	CTIO 1.0m	0.403	2004.523
2453196.5361	I	17.32 ± 0.03	CTIO 1.0m	0.411	2004.523

Table 1—Continued

HJD	Band	Magnitude	Source	Phase	Year
2453196.5446	I	17.33 ± 0.03	CTIO 1.0m	0.417	2004.523
2453196.5678	I	17.34 ± 0.03	CTIO 1.0m	0.436	2004.523
2453196.5678	I	17.31 ± 0.03	CTIO 1.0m	0.436	2004.523
2453196.5838	I	17.36 ± 0.03	CTIO 1.0m	0.449	2004.523
2453196.5960	I	17.39 ± 0.02	CTIO 1.0m	0.459	2004.523
2453196.6038	I	17.37 ± 0.02	CTIO 1.0m	0.466	2004.523
2453196.6123	I	17.45 ± 0.02	CTIO 1.0m	0.472	2004.523
2453196.6195	I	17.42 ± 0.03	CTIO 1.0m	0.478	2004.523
2453196.6268	I	17.44 ± 0.02	CTIO 1.0m	0.484	2004.523
2453196.6342	I	17.39 ± 0.03	CTIO 1.0m	0.490	2004.523
2453196.6415	I	17.52 ± 0.03	CTIO 1.0m	0.496	2004.523
2453196.6487	I	17.49 ± 0.02	CTIO 1.0m	0.502	2004.523
2453196.6563	I	17.47 ± 0.03	CTIO 1.0m	0.508	2004.523
2453196.6636	I	17.45 ± 0.03	CTIO 1.0m	0.514	2004.523
2453196.6788	I	17.42 ± 0.03	CTIO 1.0m	0.526	2004.523
2453196.6893	I	17.41 ± 0.03	CTIO 1.0m	0.535	2004.523
2453196.6965	I	17.40 ± 0.03	CTIO 1.0m	0.541	2004.523
2453196.7037	I	17.41 ± 0.03	CTIO 1.0m	0.547	2004.523
2453196.7184	I	17.30 ± 0.02	CTIO 1.0m	0.559	2004.524
2453196.7209	I	17.35 ± 0.03	CTIO 1.0m	0.561	2004.524
2453196.7352	I	17.35 ± 0.03	CTIO 1.0m	0.572	2004.524
2453196.7436	I	17.28 ± 0.03	CTIO 1.0m	0.579	2004.524
2453196.7474	I	17.28 ± 0.03	CTIO 1.0m	0.582	2004.524
2453196.7617	I	17.26 ± 0.03	CTIO 1.0m	0.594	2004.524
2453196.7690	I	17.22 ± 0.03	CTIO 1.0m	0.600	2004.524
2453197.5817	I	17.26 ± 0.02	CTIO 1.0m	0.260	2004.526
2453197.5894	R	17.71 ± 0.01	CTIO 1.0m	0.267	2004.526
2453197.5971	V	18.10 ± 0.02	CTIO 1.0m	0.273	2004.526
2453197.6048	B	18.40 ± 0.03	CTIO 1.0m	0.279	2004.526
2453197.6124	U	18.13 ± 0.08	CTIO 1.0m	0.285	2004.526
2453197.7114	I	17.25 ± 0.02	CTIO 1.0m	0.366	2004.526
2453199.4870	I	17.30 ± 0.03	CTIO 1.0m	0.809	2004.531
2453199.4943	I	17.25 ± 0.04	CTIO 1.0m	0.815	2004.531
2453199.5017	I	17.22 ± 0.04	CTIO 1.0m	0.821	2004.531
2453199.5644	I	17.30 ± 0.02	CTIO 1.0m	0.872	2004.531
2453199.5720	I	17.29 ± 0.02	CTIO 1.0m	0.878	2004.531
2453199.5795	I	17.27 ± 0.04	CTIO 1.0m	0.884	2004.531
2453199.6256	I	17.34 ± 0.04	CTIO 1.0m	0.921	2004.531
2453199.6354	I	17.39 ± 0.05	CTIO 1.0m	0.929	2004.532
2453199.6499	I	17.38 ± 0.06	CTIO 1.0m	0.941	2004.532
2453201.2230	CR	17.9 ± 0.1	AAVSO (MLF)	0.219	2004.536
2453209.2464	CR	17.8 ± 0.1	AAVSO (MLF)	0.740	2004.558
2453223.2763	CR	17.9 ± 0.1	AAVSO (MLF)	0.141	2004.596
2453237.2060	CR	17.7 ± 0.1	AAVSO (MLF)	0.461	2004.634
2453251.2566	CR	17.8 ± 0.1	AAVSO (MLF)	0.879	2004.673
2453262.2206	CR	17.8 ± 0.1	AAVSO (MLF)	0.789	2004.703

Table 1—Continued

HJD	Band	Magnitude	Source	Phase	Year
2453282.1998	CR	17.6 ± 0.1	AAVSO (MLF)	0.025	2004.758
2453288.2243	CR	17.5 ± 0.1	AAVSO (MLF)	0.921	2004.774
2453634.5334	B	18.46 ± 0.02	SMARTS 1.3m	0.348	2005.722
2453634.5399	V	17.94 ± 0.02	SMARTS 1.3m	0.353	2005.722
2453634.5447	R	17.60 ± 0.02	SMARTS 1.3m	0.357	2005.722
2453634.5488	I	17.14 ± 0.02	SMARTS 1.3m	0.360	2005.722
2453793.7702	CR	18.58 ± 0.02	AAVSO (MDJ)	0.751	2006.158
2453793.7702	CV	18.86 ± 0.02	AAVSO (MDJ)	0.751	2006.158
2453799.8147	B	18.09 ± 0.02	SMARTS 1.3m	0.663	2006.175
2453799.8212	V	17.62 ± 0.02	SMARTS 1.3m	0.668	2006.175
2453799.8260	R	17.34 ± 0.02	SMARTS 1.3m	0.672	2006.175
2453799.8303	I	16.90 ± 0.02	SMARTS 1.3m	0.676	2006.175
2453825.5522	CR	18.0 ± 0.1	AAVSO (MLF)	0.578	2006.245
2453829.6545	CR	17.5 ± 0.1	AAVSO (MLF)	0.912	2006.256
2453837.5751	CR	17.5 ± 0.1	AAVSO (MLF)	0.349	2006.278
2453855.5271	CR	17.8 ± 0.1	AAVSO (MLF)	0.937	2006.327
2453919.2248	CR	17.7 ± 0.1	AAVSO (MLF)	0.701	2006.502
2453954.2322	CR	17.2 ± 0.1	AAVSO (MLF)	0.150	2006.597
2454175.5648	CR	18.5 ± 0.1	AAVSO (MLF)	0.015	2007.203
2454214.6058	CR	17.5 ± 0.1	AAVSO (MLF)	0.742	2007.310
2454264.4516	CR	17.4 ± 0.1	AAVSO (MLF)	0.249	2007.447
2454310.2360	CR	17.9 ± 0.1	AAVSO (MLF)	0.455	2007.572
2454507.4885	CR	17.8 ± 0.1	AAVSO (MLF)	0.752	2008.112
2454513.6321	CR	17.8 ± 0.1	AAVSO (MLF)	0.744	2008.129
2454527.9007	B	18.50 ± 0.02	SMARTS 1.3m	0.340	2008.168
2454536.8221	B	17.95 ± 0.02	SMARTS 1.3m	0.590	2008.193
2454542.8568	B	18.01 ± 0.02	SMARTS 1.3m	0.494	2008.209
2454547.8175	B	18.07 ± 0.02	SMARTS 1.3m	0.525	2008.223
2454553.8468	B	18.54 ± 0.02	SMARTS 1.3m	0.425	2008.239
2454559.8413	B	18.70 ± 0.02	SMARTS 1.3m	0.296	2008.256
2454562.5227	CR	17.6 ± 0.1	AAVSO (MLF)	0.475	2008.263
2454569.7868	B	18.34 ± 0.02	SMARTS 1.3m	0.378	2008.283
2454574.7898	B	18.85 ± 0.03	SMARTS 1.3m	0.444	2008.296
2454581.7947	B	18.92 ± 0.03	SMARTS 1.3m	0.136	2008.316
2454588.7733	B	18.43 ± 0.02	SMARTS 1.3m	0.808	2008.335
2454589.6856	B	18.35 ± 0.02	SMARTS 1.3m	0.549	2008.337
2454594.7340	B	18.35 ± 0.02	SMARTS 1.3m	0.651	2008.351
2454602.8623	B	18.74 ± 0.04	SMARTS 1.3m	0.257	2008.373
2454608.8429	B	18.81 ± 0.04	SMARTS 1.3m	0.117	2008.390
2454612.1178	V	17.9 ± 0.1	AAVSO (DIL)	0.778	2008.399
2454625.6568	B	18.43 ± 0.02	SMARTS 1.3m	0.781	2008.436
2454637.7691	B	18.45 ± 0.04	SMARTS 1.3m	0.624	2008.469
2454642.7118	B	18.70 ± 0.02	SMARTS 1.3m	0.641	2008.482
2454647.6258	B	18.32 ± 0.02	SMARTS 1.3m	0.634	2008.496
2454652.5651	B	17.94 ± 0.02	SMARTS 1.3m	0.648	2008.509
2454657.6969	B	18.09 ± 0.02	SMARTS 1.3m	0.818	2008.523

Table 1—Continued

HJD	Band	Magnitude	Source	Phase	Year
2454663.6044	B	18.36 ± 0.03	SMARTS 1.3m	0.619	2008.540
2454668.4006	CR	17.8 ± 0.1	AAVSO (MLF)	0.516	2008.553
2454673.4072	CV	18.14 ± 0.02	AAVSO (PYG)	0.585	2008.566
2454674.6778	B	18.66 ± 0.02	SMARTS 1.3m	0.618	2008.570
2454683.6602	B	18.60 ± 0.02	SMARTS 1.3m	0.917	2008.595
2454685.2212	CR	17.7 ± 0.1	AAVSO (MLF)	0.186	2008.599
2454690.6428	B	18.11 ± 0.02	SMARTS 1.3m	0.591	2008.614
2454701.4197	CV	17.83 ± 0.02	AAVSO (PYG)	0.349	2008.643
2454702.4286	CV	17.93 ± 0.02	AAVSO (PYG)	0.169	2008.646
2454702.5739	B	18.03 ± 0.02	SMARTS 1.3m	0.287	2008.646
2454703.3935	CV	17.95 ± 0.02	AAVSO (PYG)	0.953	2008.649
2454704.4064	CV	17.61 ± 0.02	AAVSO (PYG)	0.776	2008.651
2454705.4003	CV	17.73 ± 0.02	AAVSO (PYG)	0.584	2008.654
2454706.4402	CV	17.99 ± 0.02	AAVSO (PYG)	0.429	2008.657
2454707.4081	CV	17.94 ± 0.02	AAVSO (PYG)	0.216	2008.660
2454707.6070	B	18.61 ± 0.02	SMARTS 1.3m	0.377	2008.660
2454709.3969	CV	17.75 ± 0.02	AAVSO (PYG)	0.832	2008.665
2454712.4106	CV	18.27 ± 0.02	AAVSO (PYG)	0.281	2008.673
2454713.2255	CR	18.2 ± 0.1	AAVSO (MLF)	0.943	2008.675
2454713.4125	CV	17.93 ± 0.02	AAVSO (PYG)	0.095	2008.676
2454723.3956	CV	17.61 ± 0.02	AAVSO (PYG)	0.208	2008.703
2454724.2045	CR	17.2 ± 0.1	AAVSO (MLF)	0.865	2008.706
2454726.5230	B	18.24 ± 0.02	SMARTS 1.3m	0.749	2008.712
2454727.9326	CV	17.72 ± 0.02	AAVSO (BHQ)	0.895	2008.716
2454728.9341	CV	17.78 ± 0.02	AAVSO (BHQ)	0.709	2008.719
2454732.5123	V	17.97 ± 0.04	SMARTS 1.3m	0.617	2008.728
2454732.5140	R	17.63 ± 0.03	SMARTS 1.3m	0.618	2008.728
2454732.5157	I	17.17 ± 0.04	SMARTS 1.3m	0.619	2008.728
2454732.5175	B	18.45 ± 0.05	SMARTS 1.3m	0.621	2008.728
2454733.3896	CV	18.26 ± 0.02	AAVSO (PYG)	0.330	2008.731
2454736.5041	B	18.58 ± 0.02	SMARTS 1.3m	0.861	2008.739
2454738.2362	CR	17.5 ± 0.1	AAVSO (MLF)	0.268	2008.744
2454738.5129	B	18.93 ± 0.02	SMARTS 1.3m	0.493	2008.745
2454740.5027	V	18.10 ± 0.06	SMARTS 1.3m	0.110	2008.750
2454740.5044	R	17.68 ± 0.04	SMARTS 1.3m	0.111	2008.750
2454740.5062	I	17.29 ± 0.07	SMARTS 1.3m	0.113	2008.750
2454740.5079	B	18.47 ± 0.06	SMARTS 1.3m	0.114	2008.750
2454742.5104	B	18.47 ± 0.02	SMARTS 1.3m	0.742	2008.756
2454745.4841	B	18.16 ± 0.02	SMARTS 1.3m	0.158	2008.764
2454746.3495	CV	18.07 ± 0.02	AAVSO (PYG)	0.861	2008.766
2454747.4891	B	18.62 ± 0.03	SMARTS 1.3m	0.787	2008.769
2454752.4958	V	17.78 ± 0.06	SMARTS 1.3m	0.856	2008.783
2454752.4975	R	17.46 ± 0.05	SMARTS 1.3m	0.857	2008.783
2454752.4992	I	17.11 ± 0.06	SMARTS 1.3m	0.859	2008.783
2454752.5010	B	18.18 ± 0.08	SMARTS 1.3m	0.860	2008.783
2454756.2098	CR	17.9 ± 0.1	AAVSO (MLF)	0.874	2008.793

Table 1—Continued

HJD	Band	Magnitude	Source	Phase	Year
2454861.0752	CV	18.56 ± 0.02	AAVSO (PKV)	0.093	2009.080
2454866.0710	CV	18.51 ± 0.02	AAVSO (PKV)	0.153	2009.094
2454881.5174	CR	17.3 ± 0.1	AAVSO (MLF)	0.705	2009.136
2454884.5797	CR	17.3 ± 0.1	AAVSO (MLF)	0.194	2009.145
2454884.7501	Sloan i'	17.16 ± 0.03	Liverpool 2.0m	0.332	2009.145
2454884.7542	B	17.88 ± 0.05	Liverpool 2.0m	0.335	2009.145
2454884.7563	V	17.46 ± 0.04	Liverpool 2.0m	0.337	2009.145
2454884.7582	V	17.45 ± 0.04	Liverpool 2.0m	0.339	2009.145
2454891.6675	Sloan i'	17.91 ± 0.02	Liverpool 2.0m	0.954	2009.164
2454891.6712	B	18.94 ± 0.06	Liverpool 2.0m	0.957	2009.164
2454891.6736	V	18.43 ± 0.06	Liverpool 2.0m	0.959	2009.164
2454891.6752	V	18.48 ± 0.06	Liverpool 2.0m	0.960	2009.164
2454893.9344	CV	17.87 ± 0.02	AAVSO (DKS)	0.796	2009.170
2454894.8580	B	18.34 ± 0.02	SMARTS 1.3m	0.546	2009.173
2454896.0435	CV	18.12 ± 0.02	AAVSO (PKV)	0.510	2009.176
2454896.2315	CV	17.76 ± 0.02	AAVSO (NMT)	0.662	2009.177
2454896.8338	B	18.22 ± 0.02	SMARTS 1.3m	0.152	2009.178
2454896.9346	CV	17.78 ± 0.02	AAVSO (DKS)	0.234	2009.178
2454898.5941	CR	17.4 ± 0.1	AAVSO (MLF)	0.582	2009.183
2454899.1651	CV	18.0 ± 0.1	AAVSO (NMT)	0.046	2009.185
2454899.8479	B	18.16 ± 0.02	SMARTS 1.3m	0.601	2009.186
2454899.9485	CV	17.49 ± 0.02	AAVSO (DKS)	0.683	2009.187
2454901.8391	B	18.38 ± 0.03	SMARTS 1.3m	0.219	2009.192
2454901.9489	CV	18.47 ± 0.02	AAVSO (DKS)	0.309	2009.192
2454902.0434	CV	18.31 ± 0.02	AAVSO (PKV)	0.385	2009.192
2454905.1590	CV	17.79 ± 0.02	AAVSO (NMT)	0.917	2009.201
2454905.8247	B	18.36 ± 0.02	SMARTS 1.3m	0.458	2009.203
2454908.8491	B	18.30 ± 0.02	SMARTS 1.3m	0.916	2009.211
2454911.0264	CV	18.00 ± 0.02	AAVSO (PKV)	0.686	2009.217
2454911.5833	CR	17.3 ± 0.1	AAVSO (MLF)	0.138	2009.219
2454911.8143	B	18.13 ± 0.02	SMARTS 1.3m	0.326	2009.219
2454912.7420	Sloan i'	17.46 ± 0.01	Liverpool 2.0m	0.080	2009.222
2454912.7460	B	18.31 ± 0.05	Liverpool 2.0m	0.083	2009.222
2454912.7481	V	17.83 ± 0.04	Liverpool 2.0m	0.085	2009.222
2454912.7500	V	17.81 ± 0.04	Liverpool 2.0m	0.086	2009.222
2454913.8012	B	18.47 ± 0.02	SMARTS 1.3m	0.940	2009.225
2454914.9116	CV	18.18 ± 0.02	AAVSO (DKS)	0.843	2009.228
2454914.9582	CV	17.78 ± 0.02	AAVSO (NMT)	0.881	2009.228
2454915.0132	CV	18.44 ± 0.02	AAVSO (PKV)	0.925	2009.228
2454915.6517	CR	17.5 ± 0.1	AAVSO (MLF)	0.444	2009.230
2454916.4988	CR	17.5 ± 0.1	AAVSO (MLF)	0.133	2009.232
2454916.7378	B	18.34 ± 0.02	SMARTS 1.3m	0.327	2009.233
2454917.6509	CR	17.5 ± 0.1	AAVSO (MLF)	0.069	2009.235
2454918.0053	CV	18.07 ± 0.02	AAVSO (PKV)	0.357	2009.236
2454918.5189	CR	17.9 ± 0.1	AAVSO (MLF)	0.774	2009.238
2454918.7660	B	19.20 ± 0.02	SMARTS 1.3m	0.975	2009.238

Table 1—Continued

HJD	Band	Magnitude	Source	Phase	Year
2454919.5610	CR	17.2 ± 0.1	AAVSO (MLF)	0.621	2009.240
2454919.5940	Sloan i'	17.36 ± 0.01	Liverpool 2.0m	0.648	2009.241
2454919.5976	B	18.24 ± 0.05	Liverpool 2.0m	0.651	2009.241
2454919.5997	V	17.70 ± 0.04	Liverpool 2.0m	0.653	2009.241
2454919.6016	V	17.71 ± 0.04	Liverpool 2.0m	0.654	2009.241
2454920.7856	B	17.96 ± 0.02	SMARTS 1.3m	0.616	2009.244
2454920.8880	CV	18.0 ± 0.1	AAVSO (DKS)	0.699	2009.244
2454921.0004	CV	18.01 ± 0.02	AAVSO (PKV)	0.791	2009.244
2454921.6982	Sloan i'	17.28 ± 0.01	Liverpool 2.0m	0.358	2009.246
2454921.7023	B	18.09 ± 0.04	Liverpool 2.0m	0.361	2009.246
2454921.7044	V	17.64 ± 0.04	Liverpool 2.0m	0.363	2009.246
2454921.7063	V	17.66 ± 0.04	Liverpool 2.0m	0.364	2009.246
2454921.9013	CV	17.92 ± 0.02	AAVSO (DKS)	0.523	2009.247
2454922.4063	CR	17.1 ± 0.1	AAVSO (MLF)	0.933	2009.248
2454922.7853	B	18.28 ± 0.02	SMARTS 1.3m	0.241	2009.249
2454923.5023	CR	17.5 ± 0.1	AAVSO (MLF)	0.824	2009.251
2454923.5767	Sloan i'	17.44 ± 0.03	Liverpool 2.0m	0.884	2009.251
2454923.5803	B	18.26 ± 0.05	Liverpool 2.0m	0.887	2009.251
2454923.5824	V	17.81 ± 0.04	Liverpool 2.0m	0.889	2009.251
2454923.5843	V	17.80 ± 0.03	Liverpool 2.0m	0.891	2009.251
2454924.7283	B	18.25 ± 0.02	SMARTS 1.3m	0.820	2009.255
2454925.7709	CV	18.16 ± 0.02	AAVSO (DKS)	0.668	2009.257
2454925.9883	CV	18.18 ± 0.02	AAVSO (PKV)	0.844	2009.258
2454926.1134	CV	18.09 ± 0.02	AAVSO (NMT)	0.946	2009.258
2454926.5486	CR	17.3 ± 0.1	AAVSO (MLF)	0.300	2009.260
2454926.5759	Sloan i'	17.20 ± 0.02	Liverpool 2.0m	0.322	2009.260
2454926.5800	B	18.04 ± 0.07	Liverpool 2.0m	0.325	2009.260
2454926.5820	V	17.58 ± 0.04	Liverpool 2.0m	0.327	2009.260
2454926.5839	V	17.59 ± 0.04	Liverpool 2.0m	0.328	2009.260
2454926.7196	B	18.23 ± 0.02	SMARTS 1.3m	0.439	2009.260
2454927.5027	CR	17.7 ± 0.1	AAVSO (MLF)	0.075	2009.262
2454928.7947	B	18.49 ± 0.02	SMARTS 1.3m	0.125	2009.266
2454930.0568	CV	17.61 ± 0.02	AAVSO (BHQ)	0.151	2009.269
2454930.8615	B	18.38 ± 0.02	SMARTS 1.3m	0.804	2009.271
2454931.1072	CV	19.35 ± 0.02	AAVSO (NMT)	0.004	2009.272
2454931.6620	Sloan i'	17.48 ± 0.03	Liverpool 2.0m	0.455	2009.274
2454931.6661	B	18.18 ± 0.08	Liverpool 2.0m	0.458	2009.274
2454931.6681	V	17.69 ± 0.06	Liverpool 2.0m	0.460	2009.274
2454931.6700	V	17.67 ± 0.06	Liverpool 2.0m	0.461	2009.274
2454932.7740	B	18.24 ± 0.03	SMARTS 1.3m	0.359	2009.277
2454933.1293	CV	17.98 ± 0.02	AAVSO (NMT)	0.647	2009.278
2454935.4532	CR	17.5 ± 0.1	AAVSO (MLF)	0.536	2009.284
2454936.7619	B	18.68 ± 0.02	SMARTS 1.3m	0.599	2009.288
2454937.5402	Sloan i'	17.78 ± 0.03	Liverpool 2.0m	0.232	2009.290
2454937.5443	B	18.88 ± 0.10	Liverpool 2.0m	0.235	2009.290
2454937.5463	V	18.24 ± 0.05	Liverpool 2.0m	0.237	2009.290

Table 1—Continued

HJD	Band	Magnitude	Source	Phase	Year
2454937.5482	V	18.20 ± 0.04	Liverpool 2.0m	0.238	2009.290
2454938.0613	V	18.50 ± 0.02	AAVSO (BHQ)	0.655	2009.291
2454938.4364	CR	18.6 ± 0.1	AAVSO (MLF)	0.960	2009.292
2454938.7630	B	18.70 ± 0.02	SMARTS 1.3m	0.226	2009.293
2454939.1014	CV	18.28 ± 0.02	AAVSO (NMT)	0.500	2009.294
2454940.5115	CR	17.6 ± 0.1	AAVSO (MLF)	0.646	2009.298
2454940.7541	B	18.26 ± 0.02	SMARTS 1.3m	0.844	2009.298
2454941.1800	CV	18.16 ± 0.02	AAVSO (PKV)	0.190	2009.300
2454942.5390	Sloan i'	17.19 ± 0.06	Liverpool 2.0m	0.294	2009.303
2454942.5472	V	17.54 ± 0.13	Liverpool 2.0m	0.301	2009.303
2454942.7979	B	18.23 ± 0.02	SMARTS 1.3m	0.505	2009.304
2454943.8966	CV	18.06 ± 0.02	AAVSO (DKS)	0.397	2009.307
2454944.1991	CV	17.96 ± 0.02	AAVSO (NMT)	0.643	2009.308
2454944.7328	CV	18.35 ± 0.02	AAVSO (DKS)	0.077	2009.309
2454945.9145	CV	18.1 ± 0.1	AAVSO (DKS)	0.037	2009.313
2454947.7751	B	18.58 ± 0.02	SMARTS 1.3m	0.549	2009.318
2454947.7996	V	18.47 ± 0.02	AAVSO (CMP)	0.569	2009.318
2454947.8423	CV	18.37 ± 0.02	AAVSO (DKS)	0.604	2009.318
2454948.9029	CV	18.01 ± 0.02	AAVSO (DKS)	0.466	2009.321
2454949.3910	CR	17.6 ± 0.1	AAVSO (MLF)	0.862	2009.322
2454949.6660	Sloan i'	17.64 ± 0.00	Liverpool 2.0m	0.086	2009.323
2454949.6701	B	18.67 ± 0.05	Liverpool 2.0m	0.089	2009.323
2454949.6721	V	18.10 ± 0.04	Liverpool 2.0m	0.091	2009.323
2454949.6740	Sloan r'	17.91 ± 0.03	Liverpool 2.0m	0.092	2009.323
2454949.7563	CV	18.07 ± 0.02	AAVSO (DKS)	0.159	2009.323
2454949.7903	B	18.60 ± 0.02	SMARTS 1.3m	0.187	2009.323
2454951.1265	CV	18.21 ± 0.02	AAVSO (NMT)	0.273	2009.327
2454951.5689	Sloan i'	17.50 ± 0.02	Liverpool 2.0m	0.632	2009.328
2454951.5729	B	18.52 ± 0.07	Liverpool 2.0m	0.635	2009.328
2454951.5749	V	17.99 ± 0.05	Liverpool 2.0m	0.637	2009.328
2454951.5768	Sloan r'	17.82 ± 0.04	Liverpool 2.0m	0.639	2009.328
2454951.7800	B	18.57 ± 0.02	SMARTS 1.3m	0.804	2009.329
2454953.6866	Sloan i'	17.63 ± 0.02	Liverpool 2.0m	0.353	2009.334
2454953.6907	B	18.55 ± 0.05	Liverpool 2.0m	0.356	2009.334
2454953.6927	V	18.02 ± 0.04	Liverpool 2.0m	0.358	2009.334
2454953.6946	Sloan r'	17.87 ± 0.03	Liverpool 2.0m	0.360	2009.334
2454953.7107	B	18.53 ± 0.02	SMARTS 1.3m	0.373	2009.334
2454954.1088	CV	18.04 ± 0.02	AAVSO (NMT)	0.696	2009.335
2454955.6663	CR	17.7 ± 0.1	AAVSO (MLF)	0.962	2009.339
2454955.7640	B	19.40 ± 0.03	SMARTS 1.3m	0.041	2009.340
2454956.3773	CR	17.7 ± 0.1	AAVSO (MLF)	0.540	2009.341
2454956.4887	Sloan i'	17.64 ± 0.03	Liverpool 2.0m	0.630	2009.342
2454956.4927	B	18.77 ± 0.16	Liverpool 2.0m	0.634	2009.342
2454956.4947	V	18.14 ± 0.06	Liverpool 2.0m	0.635	2009.342
2454956.4967	Sloan r'	17.96 ± 0.06	Liverpool 2.0m	0.637	2009.342
2454959.8068	B	18.64 ± 0.03	SMARTS 1.3m	0.327	2009.351

Table 1—Continued

HJD	Band	Magnitude	Source	Phase	Year
2454964.5124	Sloan i'	17.74 ± 0.02	Liverpool 2.0m	0.151	2009.363
2454964.5164	B	18.89 ± 0.09	Liverpool 2.0m	0.154	2009.363
2454964.5184	V	18.20 ± 0.07	Liverpool 2.0m	0.156	2009.364
2454964.5204	Sloan r'	18.03 ± 0.04	Liverpool 2.0m	0.157	2009.364
2454964.7029	B	18.67 ± 0.02	SMARTS 1.3m	0.306	2009.364
2454966.3226	CR	17.7 ± 0.1	AAVSO (MLF)	0.622	2009.368
2454966.5177	Sloan i'	17.62 ± 0.03	Liverpool 2.0m	0.780	2009.369
2454966.5216	B	18.75 ± 0.06	Liverpool 2.0m	0.784	2009.369
2454966.5236	V	18.21 ± 0.06	Liverpool 2.0m	0.785	2009.369
2454966.5256	Sloan r'	18.01 ± 0.05	Liverpool 2.0m	0.787	2009.369
2454966.6656	B	18.67 ± 0.02	SMARTS 1.3m	0.900	2009.369
2454968.3567	CR	18.1 ± 0.1	AAVSO (MLF)	0.275	2009.374
2454968.5674	Sloan i'	17.95 ± 0.02	Liverpool 2.0m	0.446	2009.375
2454968.5714	B	18.93 ± 0.05	Liverpool 2.0m	0.449	2009.375
2454968.5734	V	18.42 ± 0.06	Liverpool 2.0m	0.451	2009.375
2454968.5754	Sloan r'	18.24 ± 0.03	Liverpool 2.0m	0.452	2009.375
2454968.7377	B	18.74 ± 0.02	SMARTS 1.3m	0.584	2009.375
2454970.5467	CR	18.6 ± 0.1	AAVSO (MLF)	0.054	2009.380
2454970.7732	B	18.86 ± 0.02	SMARTS 1.3m	0.239	2009.381
2454971.4556	Sloan i'	17.71 ± 0.03	Liverpool 2.0m	0.793	2009.382
2454971.4596	B	18.68 ± 0.05	Liverpool 2.0m	0.796	2009.383
2454971.4620	V	18.12 ± 0.06	Liverpool 2.0m	0.798	2009.383
2454971.4635	Sloan r'	17.97 ± 0.04	Liverpool 2.0m	0.800	2009.383
2454972.8519	B	18.71 ± 0.02	SMARTS 1.3m	0.928	2009.386
2454972.8582	CV	18.41 ± 0.02	AAVSO (PKV)	0.933	2009.386
2454973.0938	CV	18.03 ± 0.02	AAVSO (NMT)	0.124	2009.387
2454973.1579	V	18.3 ± 0.1	AAVSO (DIL)	0.176	2009.387
2454973.9704	CV	18.07 ± 0.02	AAVSO (NMT)	0.837	2009.389
2454974.3807	CR	17.8 ± 0.1	AAVSO (MLF)	0.170	2009.391
2454974.7504	B	18.75 ± 0.02	SMARTS 1.3m	0.471	2009.392
2454975.4379	Sloan i'	18.12 ± 0.03	Liverpool 2.0m	0.029	2009.393
2454975.4419	B	19.33 ± 0.07	Liverpool 2.0m	0.032	2009.393
2454975.4439	V	18.67 ± 0.06	Liverpool 2.0m	0.034	2009.393
2454975.4458	Sloan r'	18.42 ± 0.07	Liverpool 2.0m	0.036	2009.393
2454975.7553	CV	18.29 ± 0.02	AAVSO (NMT)	0.287	2009.394
2454976.7628	V	18.05 ± 0.03	SMARTS 1.3m	0.106	2009.397
2454976.7644	R	17.72 ± 0.03	SMARTS 1.3m	0.107	2009.397
2454976.7661	I	17.26 ± 0.04	SMARTS 1.3m	0.109	2009.397
2454976.7678	B	18.55 ± 0.04	SMARTS 1.3m	0.110	2009.397
2454977.5431	Sloan i'	17.63 ± 0.02	Liverpool 2.0m	0.740	2009.399
2454977.5471	B	18.61 ± 0.06	Liverpool 2.0m	0.743	2009.399
2454977.5491	V	18.10 ± 0.05	Liverpool 2.0m	0.745	2009.399
2454977.5512	Sloan r'	17.92 ± 0.03	Liverpool 2.0m	0.747	2009.399
2454978.3128	CR	17.8 ± 0.1	AAVSO (MLF)	0.366	2009.401
2454978.3168	CR	17.6 ± 0.1	AAVSO (MLF)	0.369	2009.401
2454978.3208	CR	17.7 ± 0.1	AAVSO (MLF)	0.372	2009.401

Table 1—Continued

HJD	Band	Magnitude	Source	Phase	Year
2454978.3238	CR	17.8 ± 0.1	AAVSO (MLF)	0.374	2009.401
2454979.5858	CR	17.8 ± 0.1	AAVSO (MLF)	0.400	2009.405
2454980.7266	B	18.63 ± 0.02	SMARTS 1.3m	0.327	2009.408
2454981.2502	CV	18.32 ± 0.02	AAVSO (NMT)	0.753	2009.409
2454981.4998	Sloan i'	18.09 ± 0.04	Liverpool 2.0m	0.955	2009.410
2454981.5145	Sloan i'	18.20 ± 0.03	Liverpool 2.0m	0.967	2009.410
2454981.5186	B	19.37 ± 0.08	Liverpool 2.0m	0.971	2009.410
2454981.5205	V	18.78 ± 0.07	Liverpool 2.0m	0.972	2009.410
2454981.5225	Sloan r'	18.62 ± 0.05	Liverpool 2.0m	0.974	2009.410
2454982.6930	B	18.64 ± 0.02	SMARTS 1.3m	0.925	2009.413
2454982.7332	CV	18.57 ± 0.02	AAVSO (NMT)	0.958	2009.413
2454983.4674	B	18.57 ± 0.06	Liverpool 2.0m	0.554	2009.415
2454983.4694	V	18.01 ± 0.04	Liverpool 2.0m	0.556	2009.415
2454983.4713	Sloan r'	17.87 ± 0.03	Liverpool 2.0m	0.558	2009.415
2454983.5017	CR	17.7 ± 0.1	AAVSO (MLF)	0.582	2009.415
2454983.7407	B	18.33 ± 0.02	SMARTS 1.3m	0.777	2009.416
2454984.7141	B	18.23 ± 0.02	SMARTS 1.3m	0.568	2009.419
2454985.7129	B	17.90 ± 0.02	SMARTS 1.3m	0.379	2009.422
2454986.2017	CR	17.6 ± 0.1	AAVSO (MLF)	0.776	2009.423
2454986.4127	Sloan i'	17.66 ± 0.05	Liverpool 2.0m	0.948	2009.423
2454986.4167	B	18.56 ± 0.12	Liverpool 2.0m	0.951	2009.423
2454986.4187	V	18.11 ± 0.07	Liverpool 2.0m	0.953	2009.423
2454986.4211	Sloan r'	17.96 ± 0.04	Liverpool 2.0m	0.955	2009.423
2454986.6494	B	18.11 ± 0.02	SMARTS 1.3m	0.140	2009.424
2454987.1799	CV	17.91 ± 0.02	AAVSO (NMT)	0.571	2009.426
2454987.5817	CR	17.3 ± 0.1	AAVSO (MLF)	0.898	2009.427
2454987.7251	B	19.41 ± 0.04	SMARTS 1.3m	0.014	2009.427
2454990.7816	B	18.21 ± 0.03	SMARTS 1.3m	0.498	2009.435
2454991.7044	B	18.02 ± 0.02	SMARTS 1.3m	0.248	2009.438
2454992.4328	Sloan i'	17.33 ± 0.02	Liverpool 2.0m	0.840	2009.440
2454992.4369	B	18.19 ± 0.04	Liverpool 2.0m	0.843	2009.440
2454992.4389	V	17.70 ± 0.05	Liverpool 2.0m	0.845	2009.440
2454992.4409	Sloan r'	17.51 ± 0.03	Liverpool 2.0m	0.847	2009.440
2454992.7323	B	18.34 ± 0.02	SMARTS 1.3m	0.083	2009.441
2454993.6972	B	18.21 ± 0.02	SMARTS 1.3m	0.868	2009.443
2454994.0200	V	17.52 ± 0.02	AAVSO (DIL)	0.130	2009.444
2454994.7425	B	18.31 ± 0.02	SMARTS 1.3m	0.717	2009.446
2454995.3586	CR	17.8 ± 0.1	AAVSO (MLF)	0.218	2009.448
2454995.4596	Sloan i'	17.31 ± 0.04	Liverpool 2.0m	0.300	2009.448
2454995.4636	B	18.35 ± 0.07	Liverpool 2.0m	0.303	2009.448
2454995.4656	V	17.77 ± 0.06	Liverpool 2.0m	0.305	2009.448
2454995.4675	Sloan r'	17.60 ± 0.05	Liverpool 2.0m	0.306	2009.448
2454995.7532	B	18.29 ± 0.02	SMARTS 1.3m	0.538	2009.449
2454996.3515	CR	18.4 ± 0.1	AAVSO (MLF)	0.025	2009.451
2455002.5322	Sloan i'	18.06 ± 0.05	Liverpool 2.0m	0.047	2009.468
2455002.5362	B	19.11 ± 0.07	Liverpool 2.0m	0.051	2009.468

Table 1—Continued

HJD	Band	Magnitude	Source	Phase	Year
2455002.5382	V	18.48 ± 0.07	Liverpool 2.0m	0.052	2009.468
2455002.5402	Sloan r'	18.31 ± 0.04	Liverpool 2.0m	0.054	2009.468
2455003.2653	CR	18.2 ± 0.1	AAVSO (MLF)	0.643	2009.470
2455003.9401	CV	18.31 ± 0.02	AAVSO (NMT)	0.192	2009.471
2455004.7473	V	16.94 ± 0.02	AAVSO (PSD)	0.847	2009.474
2455004.7641	V	16.96 ± 0.02	AAVSO (PSD)	0.861	2009.474
2455004.9621	CV	18.7 ± 0.1	AAVSO (NLX)	0.022	2009.474
2455005.0724	CV	18.62 ± 0.02	AAVSO (BHQ)	0.112	2009.475
2455005.3912	CR	18.3 ± 0.1	AAVSO (MLF)	0.371	2009.475
2455005.7532	V	18.06 ± 0.02	AAVSO (SRIC)	0.665	2009.476
2455006.3362	CR	18.1 ± 0.1	AAVSO (MLF)	0.139	2009.478
2455006.4882	Sloan i'	17.70 ± 0.02	Liverpool 2.0m	0.262	2009.478
2455006.4922	B	18.76 ± 0.05	Liverpool 2.0m	0.265	2009.478
2455006.4942	V	18.22 ± 0.04	Liverpool 2.0m	0.267	2009.478
2455006.4962	Sloan r'	18.04 ± 0.03	Liverpool 2.0m	0.269	2009.478
2455007.0498	CV	18.44 ± 0.02	AAVSO (BHQ)	0.719	2009.480
2455007.2412	CR	17.8 ± 0.1	AAVSO (MLF)	0.874	2009.480
2455007.5674	B	18.69 ± 0.02	SMARTS 1.3m	0.139	2009.481
2455008.5134	B	18.53 ± 0.02	SMARTS 1.3m	0.908	2009.484
2455009.3061	CR	18.0 ± 0.1	AAVSO (MLF)	0.552	2009.486
2455009.7414	CV	17.77 ± 0.02	AAVSO (SRIC)	0.906	2009.487
2455010.3460	CR	17.7 ± 0.1	AAVSO (MLF)	0.397	2009.489
2455010.5803	B	18.62 ± 0.02	SMARTS 1.3m	0.588	2009.490
2455010.9357	CV	18.1 ± 0.1	AAVSO (NMT)	0.876	2009.491
2455011.4751	CV	17.96 ± 0.02	AAVSO (MUY)	0.315	2009.492
2455012.4913	Sloan i'	17.52 ± 0.01	Liverpool 2.0m	0.141	2009.495
2455012.4953	B	18.51 ± 0.06	Liverpool 2.0m	0.144	2009.495
2455012.4973	V	17.94 ± 0.05	Liverpool 2.0m	0.145	2009.495
2455012.4993	Sloan r'	17.76 ± 0.03	Liverpool 2.0m	0.147	2009.495
2455012.6152	B	18.56 ± 0.02	SMARTS 1.3m	0.241	2009.495
2455013.0802	CV	18.06 ± 0.02	AAVSO (NMT)	0.619	2009.496
2455013.4858	B	18.92 ± 0.05	SMARTS 1.3m	0.949	2009.498
2455014.5882	B	18.45 ± 0.02	SMARTS 1.3m	0.845	2009.501
2455014.6694	CV	17.95 ± 0.02	AAVSO (NMT)	0.911	2009.501
2455015.1362	CV	18.1 ± 0.1	AAVSO (NMT)	0.290	2009.502
2455015.1558	CV	17.95 ± 0.02	AAVSO (NMT)	0.306	2009.502
2455015.3108	CR	18.1 ± 0.1	AAVSO (MLF)	0.432	2009.503
2455018.6595	B	18.42 ± 0.03	SMARTS 1.3m	0.153	2009.512
2455019.1295	CV	17.89 ± 0.02	AAVSO (NMT)	0.535	2009.513
2455019.1392	CV	17.86 ± 0.02	AAVSO (NMT)	0.543	2009.513
2455019.2445	CR	17.3 ± 0.1	AAVSO (MLF)	0.629	2009.513
2455019.6121	B	18.63 ± 0.03	SMARTS 1.3m	0.927	2009.514
2455019.7439	CV	17.93 ± 0.02	AAVSO (NMT)	0.034	2009.515
2455020.1059	CV	18.16 ± 0.02	AAVSO (NMT)	0.329	2009.516
2455020.6297	B	18.38 ± 0.03	SMARTS 1.3m	0.754	2009.517
2455020.6710	CV	17.99 ± 0.02	AAVSO (NMT)	0.788	2009.517

Table 1—Continued

HJD	Band	Magnitude	Source	Phase	Year
2455020.7370	V	17.14 ± 0.02	AAVSO (WWL)	0.841	2009.517
2455021.1146	CV	17.96 ± 0.02	AAVSO (NMT)	0.148	2009.518
2455021.1577	CV	18.09 ± 0.02	AAVSO (NMT)	0.183	2009.519
2455021.2154	CR	17.6 ± 0.1	AAVSO (MLF)	0.230	2009.519
2455021.4884	Sloan i'	17.63 ± 0.02	Liverpool 2.0m	0.452	2009.519
2455021.4924	B	18.47 ± 0.06	Liverpool 2.0m	0.455	2009.519
2455021.4943	V	17.95 ± 0.07	Liverpool 2.0m	0.457	2009.519
2455021.4963	Sloan r'	17.83 ± 0.04	Liverpool 2.0m	0.459	2009.519
2455021.6017	B	18.44 ± 0.02	SMARTS 1.3m	0.544	2009.520
2455021.6496	CV	18.11 ± 0.02	AAVSO (NMT)	0.583	2009.520
2455022.2654	CR	17.6 ± 0.1	AAVSO (MLF)	0.083	2009.522
2455022.5897	B	18.45 ± 0.02	SMARTS 1.3m	0.347	2009.522
2455022.6491	CV	17.9 ± 0.1	AAVSO (NMT)	0.395	2009.523
2455022.7025	CV	18.05 ± 0.02	AAVSO (NMT)	0.439	2009.523
2455023.2803	CR	18.0 ± 0.1	AAVSO (MLF)	0.908	2009.524
2455023.5690	B	18.57 ± 0.02	SMARTS 1.3m	0.143	2009.525
2455023.6563	CV	18.04 ± 0.02	AAVSO (NMT)	0.214	2009.525
2455023.7081	CV	18.28 ± 0.02	AAVSO (NMT)	0.256	2009.526
2455023.7447	CV	18.17 ± 0.02	AAVSO (NMT)	0.286	2009.526
2455024.2232	CR	17.4 ± 0.1	AAVSO (MLF)	0.675	2009.527
2455024.7032	CV	17.91 ± 0.02	AAVSO (NMT)	0.065	2009.528
2455025.0929	CV	18.14 ± 0.02	AAVSO (NMT)	0.381	2009.529
2455025.1363	CV	18.05 ± 0.02	AAVSO (NMT)	0.417	2009.529
2455025.2142	CR	17.9 ± 0.1	AAVSO (MLF)	0.480	2009.530
2455025.6573	CV	18.28 ± 0.02	AAVSO (NMT)	0.840	2009.531
2455026.1473	CV	17.84 ± 0.02	AAVSO (NMT)	0.238	2009.532
2455026.3724	CR	18.05 ± 0.02	AAVSO (BZU)	0.421	2009.533
2455026.4402	Sloan i'	17.69 ± 0.01	Liverpool 2.0m	0.476	2009.533
2455026.4443	B	18.60 ± 0.06	Liverpool 2.0m	0.479	2009.533
2455026.4463	V	18.11 ± 0.05	Liverpool 2.0m	0.481	2009.533
2455026.4484	Sloan r'	17.97 ± 0.03	Liverpool 2.0m	0.483	2009.533
2455026.6593	CV	17.92 ± 0.02	AAVSO (NMT)	0.654	2009.534
2455026.6939	CV	18.0 ± 0.1	AAVSO (NMT)	0.682	2009.534
2455026.9864	CV	18.2 ± 0.1	AAVSO (NLX)	0.920	2009.535
2455027.2600	CR	17.5 ± 0.1	AAVSO (MLF)	0.142	2009.535
2455027.6750	CV	18.22 ± 0.02	AAVSO (NMT)	0.480	2009.536
2455028.0956	CV	17.88 ± 0.02	AAVSO (NMT)	0.821	2009.538
2455028.1546	CV	17.9 ± 0.1	AAVSO (NMT)	0.869	2009.538
2455028.2690	CR	18.6 ± 0.1	AAVSO (MLF)	0.962	2009.538
2455028.7536	CV	17.57 ± 0.02	AAVSO (SRIC)	0.356	2009.539
2455029.2459	CR	17.3 ± 0.1	AAVSO (MLF)	0.756	2009.541
2455029.6240	B	18.71 ± 0.02	SMARTS 1.3m	0.063	2009.542
2455029.6289	CV	18.2 ± 0.1	AAVSO (NMT)	0.067	2009.542
2455030.6482	CV	18.33 ± 0.02	AAVSO (NMT)	0.896	2009.545
2455031.2258	CR	17.7 ± 0.1	AAVSO (MLF)	0.365	2009.546
2455031.4477	CV	17.95 ± 0.02	AAVSO (PYG)	0.545	2009.547

Table 1—Continued

HJD	Band	Magnitude	Source	Phase	Year
2455032.0822	CV	18.19 ± 0.02	AAVSO (NMT)	0.061	2009.548
2455032.2137	CR	17.6 ± 0.1	AAVSO (MLF)	0.168	2009.549
2455032.4878	Sloan i'	17.47 ± 0.02	Liverpool 2.0m	0.391	2009.550
2455032.4918	B	18.41 ± 0.05	Liverpool 2.0m	0.394	2009.550
2455032.4938	V	17.89 ± 0.04	Liverpool 2.0m	0.396	2009.550
2455032.4958	Sloan r'	17.77 ± 0.04	Liverpool 2.0m	0.397	2009.550
2455032.8893	CV	17.98 ± 0.02	AAVSO (NMT)	0.717	2009.551
2455032.9295	CV	17.92 ± 0.02	AAVSO (NMT)	0.750	2009.551
2455033.1077	CV	17.99 ± 0.02	AAVSO (NMT)	0.894	2009.551
2455033.2126	CR	18.7 ± 0.1	AAVSO (MLF)	0.980	2009.552
2455033.8991	CV	18.02 ± 0.02	AAVSO (NMT)	0.538	2009.553
2455034.2005	CR	17.4 ± 0.1	AAVSO (MLF)	0.783	2009.554
2455034.6668	CV	18.35 ± 0.02	AAVSO (NMT)	0.161	2009.556
2455034.7064	CV	17.78 ± 0.02	AAVSO (SRIC)	0.194	2009.556
2455035.2465	CR	17.6 ± 0.1	AAVSO (MLF)	0.633	2009.557
2455035.4884	Sloan i'	17.47 ± 0.02	Liverpool 2.0m	0.829	2009.558
2455035.4923	B	18.49 ± 0.05	Liverpool 2.0m	0.832	2009.558
2455035.4943	V	17.95 ± 0.05	Liverpool 2.0m	0.834	2009.558
2455035.4963	Sloan r'	17.77 ± 0.04	Liverpool 2.0m	0.836	2009.558
2455035.8740	CV	17.6 ± 0.1	AAVSO (NLX)	0.142	2009.559
2455036.1247	CV	17.84 ± 0.02	AAVSO (NMT)	0.346	2009.560
2455036.1954	CR	17.4 ± 0.1	AAVSO (MLF)	0.404	2009.560
2455036.6378	B	18.44 ± 0.02	SMARTS 1.3m	0.763	2009.561
2455036.6485	CV	18.07 ± 0.02	AAVSO (NMT)	0.772	2009.561
2455036.9427	CV	19.12 ± 0.02	AAVSO (NMT)	0.011	2009.562
2455037.1186	CV	18.07 ± 0.02	AAVSO (NMT)	0.154	2009.562
2455037.6971	CV	17.84 ± 0.02	AAVSO (NMT)	0.624	2009.564
2455037.9416	CV	18.05 ± 0.02	AAVSO (NMT)	0.823	2009.565
2455037.9820	CV	17.95 ± 0.02	AAVSO (NMT)	0.856	2009.565
2455038.0482	CV	18.05 ± 0.02	AAVSO (NMT)	0.909	2009.565
2455038.2052	CR	18.2 ± 0.1	AAVSO (MLF)	0.037	2009.565
2455038.6556	CV	18.16 ± 0.02	AAVSO (NMT)	0.403	2009.566
2455039.0178	CV	17.98 ± 0.02	AAVSO (NMT)	0.697	2009.567
2455039.2101	CR	17.5 ± 0.1	AAVSO (MLF)	0.854	2009.568
2455039.9326	CV	18.14 ± 0.02	AAVSO (NMT)	0.441	2009.570
2455040.2301	CR	17.4 ± 0.1	AAVSO (MLF)	0.682	2009.571
2455040.5758	B	19.05 ± 0.02	SMARTS 1.3m	0.963	2009.572
2455041.0937	CV	18.09 ± 0.02	AAVSO (NMT)	0.384	2009.573
2455041.2130	CR	17.9 ± 0.1	AAVSO (MLF)	0.481	2009.573
2455041.6488	B	18.43 ± 0.02	SMARTS 1.3m	0.835	2009.575
2455042.5988	B	18.58 ± 0.02	SMARTS 1.3m	0.607	2009.577
2455044.9893	V	17.22 ± 0.02	AAVSO (BHQ)	0.550	2009.584
2455046.6768	B	18.56 ± 0.03	SMARTS 1.3m	0.921	2009.588
2455046.9893	V	17.96 ± 0.02	AAVSO (BHQ)	0.175	2009.589
2455047.5894	CV	17.94 ± 0.02	AAVSO (MJLE)	0.663	2009.591
2455048.0763	CV	18.22 ± 0.02	AAVSO (NMT)	0.059	2009.592

Table 1—Continued

HJD	Band	Magnitude	Source	Phase	Year
2455048.4355	Sloan i'	17.52 ± 0.01	Liverpool 2.0m	0.350	2009.593
2455048.4395	B	18.45 ± 0.06	Liverpool 2.0m	0.354	2009.593
2455048.4414	V	17.93 ± 0.07	Liverpool 2.0m	0.355	2009.593
2455048.4434	Sloan r'	17.75 ± 0.04	Liverpool 2.0m	0.357	2009.593
2455048.4733	Sloan i'	17.57 ± 0.02	Liverpool 2.0m	0.381	2009.593
2455048.4772	B	18.52 ± 0.07	Liverpool 2.0m	0.384	2009.593
2455048.4791	V	17.96 ± 0.06	Liverpool 2.0m	0.386	2009.593
2455048.4811	Sloan r'	17.78 ± 0.03	Liverpool 2.0m	0.388	2009.593
2455048.5534	CV	18.27 ± 0.02	AAVSO (MJLE)	0.446	2009.594
2455048.6338	B	18.47 ± 0.03	SMARTS 1.3m	0.512	2009.594
2455048.6900	CV	17.97 ± 0.02	AAVSO (NMT)	0.557	2009.594
2455049.9723	V	18.06 ± 0.02	AAVSO (BHQ)	0.599	2009.597
2455049.9777	CV	17.94 ± 0.02	AAVSO (NMT)	0.604	2009.597
2455050.0707	CV	17.8 ± 0.1	AAVSO (NMT)	0.679	2009.598
2455050.5672	CV	18.22 ± 0.02	AAVSO (MJLE)	0.083	2009.599
2455050.8958	CV	17.96 ± 0.02	AAVSO (NMT)	0.350	2009.600
2455051.9287	CV	17.95 ± 0.02	AAVSO (NMT)	0.189	2009.603
2455051.9728	CV	17.85 ± 0.02	AAVSO (NMT)	0.225	2009.603
2455052.4291	Sloan i'	17.22 ± 0.03	Liverpool 2.0m	0.596	2009.604
2455052.4331	B	18.06 ± 0.05	Liverpool 2.0m	0.599	2009.604
2455052.4350	V	17.60 ± 0.03	Liverpool 2.0m	0.601	2009.604
2455052.4370	Sloan r'	17.47 ± 0.03	Liverpool 2.0m	0.602	2009.604
2455053.1989	CR	17.4 ± 0.1	AAVSO (MLF)	0.222	2009.606
2455053.5649	CV	18.05 ± 0.02	AAVSO (MJLE)	0.519	2009.607
2455053.5934	B	18.19 ± 0.02	SMARTS 1.3m	0.542	2009.607
2455053.6484	V	17.43 ± 0.02	AAVSO (ARJ)	0.587	2009.608
2455053.6981	V	17.80 ± 0.02	AAVSO (MGW)	0.627	2009.608
2455054.4497	Sloan i'	17.38 ± 0.02	Liverpool 2.0m	0.238	2009.610
2455054.4556	V	17.84 ± 0.06	Liverpool 2.0m	0.243	2009.610
2455054.4575	Sloan r'	17.64 ± 0.03	Liverpool 2.0m	0.244	2009.610
2455054.5229	B	18.29 ± 0.02	SMARTS 1.3m	0.297	2009.610
2455054.6143	V	18.05 ± 0.02	AAVSO (ARJ)	0.372	2009.610
2455055.2948	CR	17.8 ± 0.1	AAVSO (MLF)	0.925	2009.612
2455055.9509	CV	17.92 ± 0.02	AAVSO (NMT)	0.458	2009.614
2455056.6351	CV	18.84 ± 0.02	AAVSO (NMT)	0.014	2009.616
2455056.9922	CV	17.97 ± 0.02	AAVSO (NMT)	0.304	2009.617
2455057.2436	CR	17.5 ± 0.1	AAVSO (MLF)	0.508	2009.617
2455057.5625	CV	17.99 ± 0.02	AAVSO (MJLE)	0.768	2009.618
2455057.5702	B	18.34 ± 0.02	SMARTS 1.3m	0.774	2009.618
2455057.9987	CV	18.04 ± 0.02	AAVSO (NMT)	0.122	2009.619
2455058.5564	CV	17.96 ± 0.02	AAVSO (MJLE)	0.575	2009.621
2455058.5892	B	18.18 ± 0.03	SMARTS 1.3m	0.602	2009.621
2455058.6450	CV	17.9 ± 0.1	AAVSO (NMT)	0.647	2009.621
2455059.1964	CR	17.3 ± 0.1	AAVSO (MLF)	0.095	2009.623
2455059.5504	CV	18.06 ± 0.02	AAVSO (MJLE)	0.383	2009.624
2455059.6251	CV	18.02 ± 0.02	AAVSO (NMT)	0.444	2009.624

Table 1—Continued

HJD	Band	Magnitude	Source	Phase	Year
2455060.5543	CV	18.19 ± 0.02	AAVSO (MJLE)	0.199	2009.626
2455060.6529	CV	18.29 ± 0.02	AAVSO (NMT)	0.279	2009.627
2455061.2272	CR	17.6 ± 0.1	AAVSO (MLF)	0.746	2009.628
2455061.5862	CV	19.03 ± 0.02	AAVSO (MJLE)	0.037	2009.629
2455061.6248	CV	18.7 ± 0.1	AAVSO (NMT)	0.069	2009.629
2455062.2111	CR	17.6 ± 0.1	AAVSO (MLF)	0.545	2009.631
2455062.3873	Sloan i'	17.58 ± 0.02	Liverpool 2.0m	0.688	2009.631
2455062.3912	B	18.59 ± 0.05	Liverpool 2.0m	0.692	2009.631
2455062.3932	V	18.06 ± 0.05	Liverpool 2.0m	0.693	2009.631
2455062.3951	Sloan r'	17.87 ± 0.03	Liverpool 2.0m	0.695	2009.631
2455063.9631	CV	18.49 ± 0.02	AAVSO (NMT)	0.969	2009.636
2455064.2179	CR	17.7 ± 0.1	AAVSO (MLF)	0.176	2009.636
2455064.5759	CV	18.35 ± 0.02	AAVSO (MJLE)	0.467	2009.637
2455065.2878	CR	18.3 ± 0.1	AAVSO (MLF)	0.046	2009.639
2455066.2857	CR	17.6 ± 0.1	AAVSO (MLF)	0.856	2009.642
2455066.4128	Sloan i'	17.99 ± 0.02	Liverpool 2.0m	0.960	2009.642
2455066.4165	B	18.91 ± 0.06	Liverpool 2.0m	0.963	2009.642
2455066.4183	V	18.45 ± 0.07	Liverpool 2.0m	0.964	2009.642
2455066.4201	Sloan r'	18.33 ± 0.05	Liverpool 2.0m	0.966	2009.642
2455066.4247	CV	18.15 ± 0.02	AAVSO (PYG)	0.969	2009.643
2455067.5596	CV	18.23 ± 0.02	AAVSO (MJLE)	0.892	2009.646
2455068.2335	CR	17.8 ± 0.1	AAVSO (MLF)	0.439	2009.647
2455068.5745	CV	18.08 ± 0.02	AAVSO (MJLE)	0.716	2009.648
2455069.2264	CR	17.6 ± 0.1	AAVSO (MLF)	0.246	2009.650
2455070.2023	CR	18.4 ± 0.1	AAVSO (MLF)	0.039	2009.653
2455070.5523	CV	18.35 ± 0.02	AAVSO (MJLE)	0.324	2009.654
2455072.1991	CR	17.4 ± 0.1	AAVSO (MLF)	0.662	2009.658
2455073.2380	CR	17.8 ± 0.1	AAVSO (MLF)	0.506	2009.661
2455073.5008	B	18.65 ± 0.02	SMARTS 1.3m	0.720	2009.662
2455075.2009	CR	18.3 ± 0.1	AAVSO (MLF)	0.101	2009.667
2455076.2258	CR	18.0 ± 0.1	AAVSO (MLF)	0.934	2009.669
2455076.5441	B	19.12 ± 0.05	SMARTS 1.3m	0.193	2009.670
2455077.2117	CR	18.4 ± 0.1	AAVSO (MLF)	0.735	2009.672
2455078.2106	CR	17.9 ± 0.1	AAVSO (MLF)	0.547	2009.675
2455078.5161	B	18.76 ± 0.03	SMARTS 1.3m	0.795	2009.676
2455079.2145	CR	17.8 ± 0.1	AAVSO (MLF)	0.363	2009.678
2455079.4997	B	19.02 ± 0.08	SMARTS 1.3m	0.595	2009.678
2455079.5013	I	17.70 ± 0.06	SMARTS 1.3m	0.596	2009.678
2455079.5030	R	18.16 ± 0.05	SMARTS 1.3m	0.597	2009.678
2455079.5045	V	18.55 ± 0.07	SMARTS 1.3m	0.599	2009.678
2455080.2844	CR	17.8 ± 0.1	AAVSO (MLF)	0.232	2009.680
2455082.3062	CR	17.9 ± 0.1	AAVSO (MLF)	0.875	2009.686
2455083.5801	B	18.90 ± 0.02	SMARTS 1.3m	0.911	2009.689
2455084.1990	CR	17.8 ± 0.1	AAVSO (MLF)	0.414	2009.691
2455084.5060	CV	18.22 ± 0.02	AAVSO (MJLE)	0.663	2009.692
2455084.5538	B	18.94 ± 0.02	SMARTS 1.3m	0.702	2009.692

Table 1—Continued

HJD	Band	Magnitude	Source	Phase	Year
2455085.3689	Sloan i'	17.80 ± 0.02	Liverpool 2.0m	0.364	2009.694
2455085.3725	B	18.86 ± 0.07	Liverpool 2.0m	0.367	2009.694
2455085.3743	V	18.26 ± 0.06	Liverpool 2.0m	0.369	2009.694
2455085.3761	Sloan r'	18.07 ± 0.04	Liverpool 2.0m	0.370	2009.694
2455087.1957	CR	17.5 ± 0.1	AAVSO (MLF)	0.849	2009.699
2455088.3633	Sloan i'	17.72 ± 0.02	Liverpool 2.0m	0.798	2009.703
2455088.3669	B	18.79 ± 0.06	Liverpool 2.0m	0.801	2009.703
2455088.3688	V	18.22 ± 0.05	Liverpool 2.0m	0.802	2009.703
2455088.3706	Sloan r'	18.03 ± 0.03	Liverpool 2.0m	0.804	2009.703
2455088.5436	CV	18.73 ± 0.02	AAVSO (MJLE)	0.944	2009.703
2455089.4934	B	18.83 ± 0.02	SMARTS 1.3m	0.716	2009.706
2455089.5215	CV	18.46 ± 0.02	AAVSO (MJLE)	0.739	2009.706
2455090.2004	CR	17.3 ± 0.1	AAVSO (MLF)	0.291	2009.708
2455091.2563	CR	18.0 ± 0.1	AAVSO (MLF)	0.149	2009.710
2455093.2561	CR	17.7 ± 0.1	AAVSO (MLF)	0.774	2009.716
2455093.5311	CV	18.90 ± 0.02	AAVSO (MJLE)	0.997	2009.717
2455094.2020	CR	17.9 ± 0.1	AAVSO (MLF)	0.543	2009.719
2455095.2039	CR	17.7 ± 0.1	AAVSO (MLF)	0.357	2009.721
2455095.5229	CV	18.15 ± 0.02	AAVSO (MJLE)	0.616	2009.722
2455096.4845	B	18.47 ± 0.02	SMARTS 1.3m	0.397	2009.725
2455096.5228	CV	18.27 ± 0.02	AAVSO (MJLE)	0.429	2009.725
2455100.5070	B	18.10 ± 0.02	SMARTS 1.3m	0.666	2009.736
2455101.2124	CR	17.6 ± 0.1	AAVSO (MLF)	0.240	2009.738
2455101.5017	B	18.23 ± 0.02	SMARTS 1.3m	0.475	2009.739
2455102.2203	CR	17.9 ± 0.1	AAVSO (MLF)	0.059	2009.741
2455102.5093	CV	18.15 ± 0.02	AAVSO (MJLE)	0.293	2009.741
2455103.4949	B	18.25 ± 0.03	SMARTS 1.3m	0.094	2009.744
2455103.5022	CV	17.98 ± 0.02	AAVSO (MJLE)	0.100	2009.744
2455104.4800	B	18.27 ± 0.03	SMARTS 1.3m	0.895	2009.747
2455104.5081	CV	18.18 ± 0.02	AAVSO (MJLE)	0.918	2009.747
2455105.4955	B	18.45 ± 0.03	SMARTS 1.3m	0.720	2009.749
2455105.5190	CV	18.02 ± 0.02	AAVSO (MJLE)	0.739	2009.750
2455106.4936	B	18.37 ± 0.03	SMARTS 1.3m	0.531	2009.752
2455106.4939	CV	18.3 ± 0.1	AAVSO (MJLE)	0.532	2009.752
2455108.5038	CV	18.3 ± 0.1	AAVSO (MJLE)	0.165	2009.758
2455109.4822	B	19.09 ± 0.06	SMARTS 1.3m	0.960	2009.760
2455110.5066	CV	18.26 ± 0.02	AAVSO (MJLE)	0.792	2009.763
2455110.8767	V	17.67 ± 0.02	AAVSO (BHQ)	0.093	2009.764
2455113.4882	B	18.68 ± 0.06	SMARTS 1.3m	0.215	2009.771
2455114.4997	B	19.40 ± 0.04	SMARTS 1.3m	0.037	2009.774
2455123.2137	CR	17.8 ± 0.1	AAVSO (MLF)	0.119	2009.798
2455123.4897	CV	18.4 ± 0.1	AAVSO (MJLE)	0.343	2009.799
2455124.4856	CV	18.5 ± 0.1	AAVSO (MJLE)	0.152	2009.801
2455126.4825	CV	18.6 ± 0.1	AAVSO (MJLE)	0.775	2009.807
2455139.7083	Visual	>12.0 ± 0.1	AAVSO(LMK)	0.523	2009.843
2455141.8861	Visual	>11.5 ± 0.1	AAVSO (KSH)	0.293	2009.849

Table 1—Continued

HJD	Band	Magnitude	Source	Phase	Year
2455158.9458	CV	>8.6 ± 0.1	AAVSO(DKS)	0.156	2009.896
2455159.9875	CV	>8.6 ± 0.1	AAVSO(DKS)	0.003	2009.899
2455161.0292	CV	>8.6 ± 0.1	AAVSO(DKS)	0.849	2009.902
2455162.1792	CV	>8.6 ± 0.1	AAVSO(DKS)	0.784	2009.905
2455163.1958	CV	>8.6 ± 0.1	AAVSO(DKS)	0.610	2009.907
2455163.6125	CV	>8.6 ± 0.1	AAVSO(DKS)	0.949	2009.909
2455165.3625	CV	>8.6 ± 0.1	AAVSO(DKS)	0.371	2009.913
2455165.9708	CV	>8.6 ± 0.1	AAVSO(DKS)	0.865	2009.915
2455193.1556	Visual	>14.0 ± 0.1	AAVSO(LMK)	0.957	2009.989
2455194.1535	Visual	>14.3 ± 0.1	AAVSO(LMK)	0.769	2009.992
2455195.9635	V	>17.4 ± 0.1	AAVSO (HBB)	0.239	2009.997
2455200.9643	V	17.6 ± 0.1	AAVSO (HBB)	0.303	2010.011
2455201.9701	V	17.40 ± 0.02	AAVSO (HBB)	0.120	2010.014
2455202.9553	V	17.75 ± 0.02	AAVSO (HBB)	0.921	2010.016
2455203.9426	V	17.6 ± 0.1	AAVSO (HBB)	0.723	2010.019
2455206.9348	CV	18.4 ± 0.1	AAVSO (MJLE)	0.154	2010.027
2455207.9399	CV	19.4 ± 0.1	AAVSO (MJLE)	0.971	2010.030
2455208.9373	V	17.8 ± 0.1	AAVSO (HBB)	0.782	2010.033
2455209.9455	V	17.6 ± 0.1	AAVSO (HBB)	0.601	2010.035
2455210.9441	CV	18.15 ± 0.02	AAVSO (MJLE)	0.413	2010.038
2455210.9527	V	18.2 ± 0.1	AAVSO (HBB)	0.420	2010.038
2455211.9532	CV	18.2 ± 0.1	AAVSO (MJLE)	0.233	2010.041
2455214.7784	Sloan i'	17.54 ± 0.04	Liverpool 2.0m	0.529	2010.049
2455214.7820	B	18.49 ± 0.09	Liverpool 2.0m	0.531	2010.049
2455214.7838	V	17.88 ± 0.06	Liverpool 2.0m	0.533	2010.049
2455214.7857	Sloan r'	17.75 ± 0.04	Liverpool 2.0m	0.534	2010.049
2455215.9105	CV	18.4 ± 0.1	AAVSO (MJLE)	0.449	2010.052
2455215.9524	V	17.7 ± 0.1	AAVSO (HBB)	0.483	2010.052
2455216.9534	V	17.7 ± 0.1	AAVSO (HBB)	0.296	2010.055
2455217.7734	Sloan i'	18.07 ± 0.03	Liverpool 2.0m	0.962	2010.057
2455217.7770	B	19.18 ± 0.08	Liverpool 2.0m	0.965	2010.057
2455217.7789	V	18.59 ± 0.05	Liverpool 2.0m	0.967	2010.057
2455217.7807	Sloan r'	18.48 ± 0.06	Liverpool 2.0m	0.968	2010.057
2455219.7638	Sloan i'	17.73 ± 0.05	Liverpool 2.0m	0.580	2010.062
2455219.7674	B	18.76 ± 0.07	Liverpool 2.0m	0.583	2010.062
2455219.7693	V	18.15 ± 0.07	Liverpool 2.0m	0.584	2010.062
2455219.7711	Sloan r'	17.97 ± 0.05	Liverpool 2.0m	0.586	2010.062
2455219.9308	CV	18.32 ± 0.02	AAVSO (MJLE)	0.716	2010.063
2455222.7671	Sloan i'	18.29 ± 0.04	Liverpool 2.0m	0.021	2010.071
2455222.7708	B	19.46 ± 0.08	Liverpool 2.0m	0.024	2010.071
2455222.7726	V	18.74 ± 0.09	Liverpool 2.0m	0.025	2010.071
2455222.7744	Sloan r'	18.55 ± 0.08	Liverpool 2.0m	0.026	2010.071
2455222.9351	CV	18.16 ± 0.02	AAVSO (MJLE)	0.157	2010.071
2455222.9628	V	18.3 ± 0.1	AAVSO (HBB)	0.180	2010.071
2455223.9232	CV	18.6 ± 0.1	AAVSO (MJLE)	0.960	2010.074
2455223.9473	V	18.2 ± 0.1	AAVSO (HBB)	0.980	2010.074

Table 1—Continued

HJD	Band	Magnitude	Source	Phase	Year
2455224.1271	Visual	$>16.5 \pm 0.1$	AAVSO(LMK)	0.126	2010.074
2455224.1649	V	$>15.0 \pm 0.1$	ASAS-3N	0.156	2010.074
2455224.3438	CV	$>9.2 \pm 0.10$	VSLOJ(Wny)	0.302	2010.075
2455224.9385	V	7.85 ± 0.10	AAVSO(HBB)	0.785	2010.076
2455224.9720	Visual	8.1 ± 0.3	AAVSO(SCK)	0.812	2010.077
2455224.9751	V	7.98 ± 0.01	AAVSO(DKS)	0.815	2010.077

Table 2. Average Magnitudes, Colors, and Fluxes

Quantity	Date Range	Average	RMS	Number
U	2004.5	18.13	...	1
B	2001.6-2010.1	18.45	0.26	145
V	2000.4-2010.1	18.01	0.29	229
R	2001.2-2009.8	17.67	0.26	127
I	2001.5-2009.7	17.35	0.14	115
Sloan r'	2009.3-2010.1	17.86	0.18	26
Sloan i'	2009.1-2010.1	17.53	0.20	33
U-B	2004.5	-0.27	...	1
B-V	2005.7-2010.1	0.54	0.06	34
V-R	2001.2-2009.4	0.34	0.05	10
R-I	2004.4-2009.7	0.46	0.09	7
r'-i'	2009.3-2010.1	0.29	0.07	33
B	2001.6-2006.2	18.45	0.29	11
B	2008.1-2008.8	18.42	0.28	34
B	2009.1-2009.8	18.46	0.26	98
B	2010.0-2010.1	18.63	0.20	2
V	2000.4-2001.7	18.07	0.33	12
V	2003.4-2006.2	18.10	0.40	9
V	2008.3-2008.8	17.91	0.20	18
V	2009.1-2009.2	17.86	0.37	9
V	2009.2-2009.3	17.92	0.26	25
V	2009.3-2009.4	18.12	0.19	23
V	2009.4-2009.5	17.93	0.46	17
V	2009.5-2009.6	17.98	0.22	58
V	2009.6-2009.7	18.06	0.22	27
V	2009.7-2009.9	18.28	0.18	13
V	2010.0-2010.1	17.97	0.33	17
$F_{B,18}^{1,5}$	2001.6-2006.2	0.58	0.20	11
$F_{B,18}^{1,5}$	2008.1-2008.8	0.60	0.23	34
$F_{B,18}^{1,5}$	2009.1-2010.1	0.56	0.20	100
$F_{B,18}^{1,5}$	1999.2-2010.1	0.58	0.05 ^a	145
$F_{B,18}^{1,5}$	1987.4-1992.2	0.50	0.03 ^a	26
$F_{B,18}^{1,5}$	1979.5-1987.4	0.66	0.05 ^a	4
$F_{B,18}^{1,5}$	1969.1-1979.5	0.55	0.12 ^a	2
$F_{B,18}^{1,5}$	1954.5	0.33	...	1

^aThe quoted value is not the RMS scatter of the quantity, but rather is the one-sigma uncertainty in the average value.

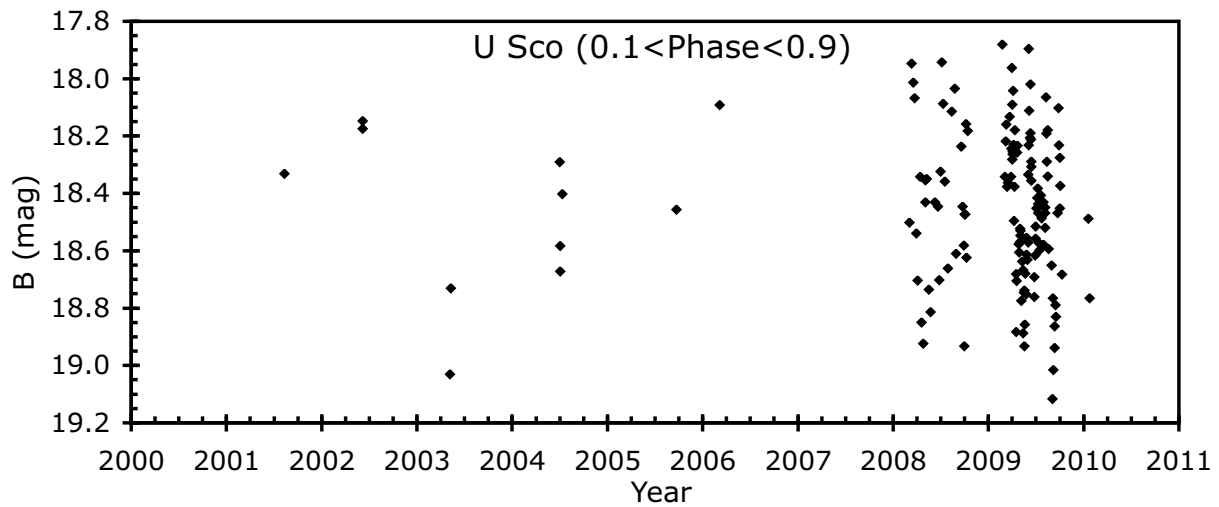


Fig. 1.— U Sco light curve in B, from 2000 to 2010. The B-band light comes almost entirely from the disk and is a measure of the mass accretion rate. This light curve does not include observations within 0.1 phase of the eclipses. The light curve shows substantial short-term changes but no significant long-term variations.

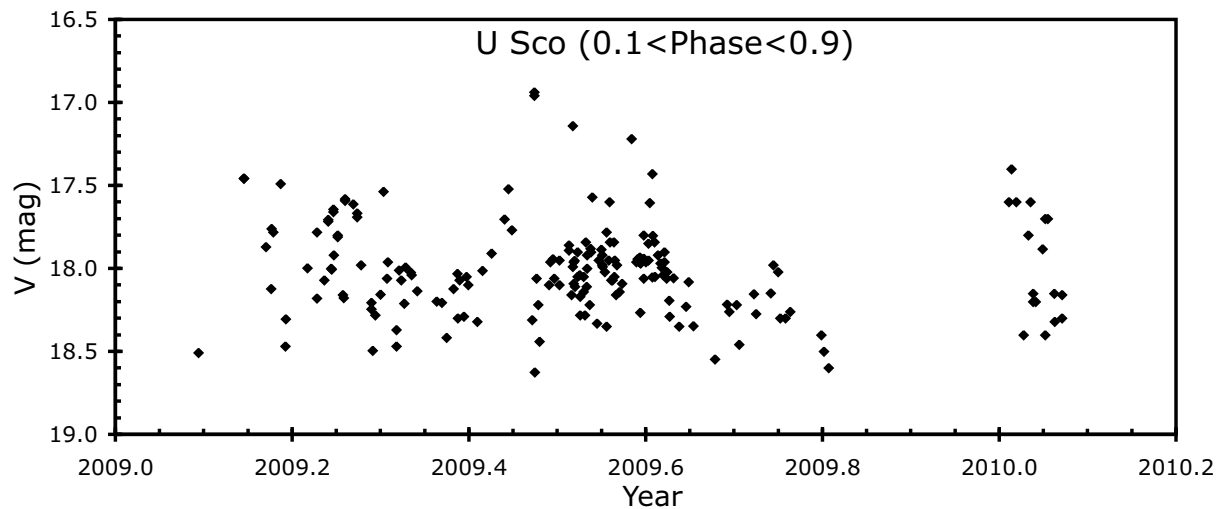


Fig. 2.— U Sco light curve in V for the last year before eruption. The observations within 0.1 phase of eclipses are not included so as to concentrate on changes of the system brightness alone. U Sco shows frequent short timescale variations, but long-term changes are apparently not significant. In particular, U Sco does not show any pre-eruption rise or dip on timescales from one day to years before the eruption.

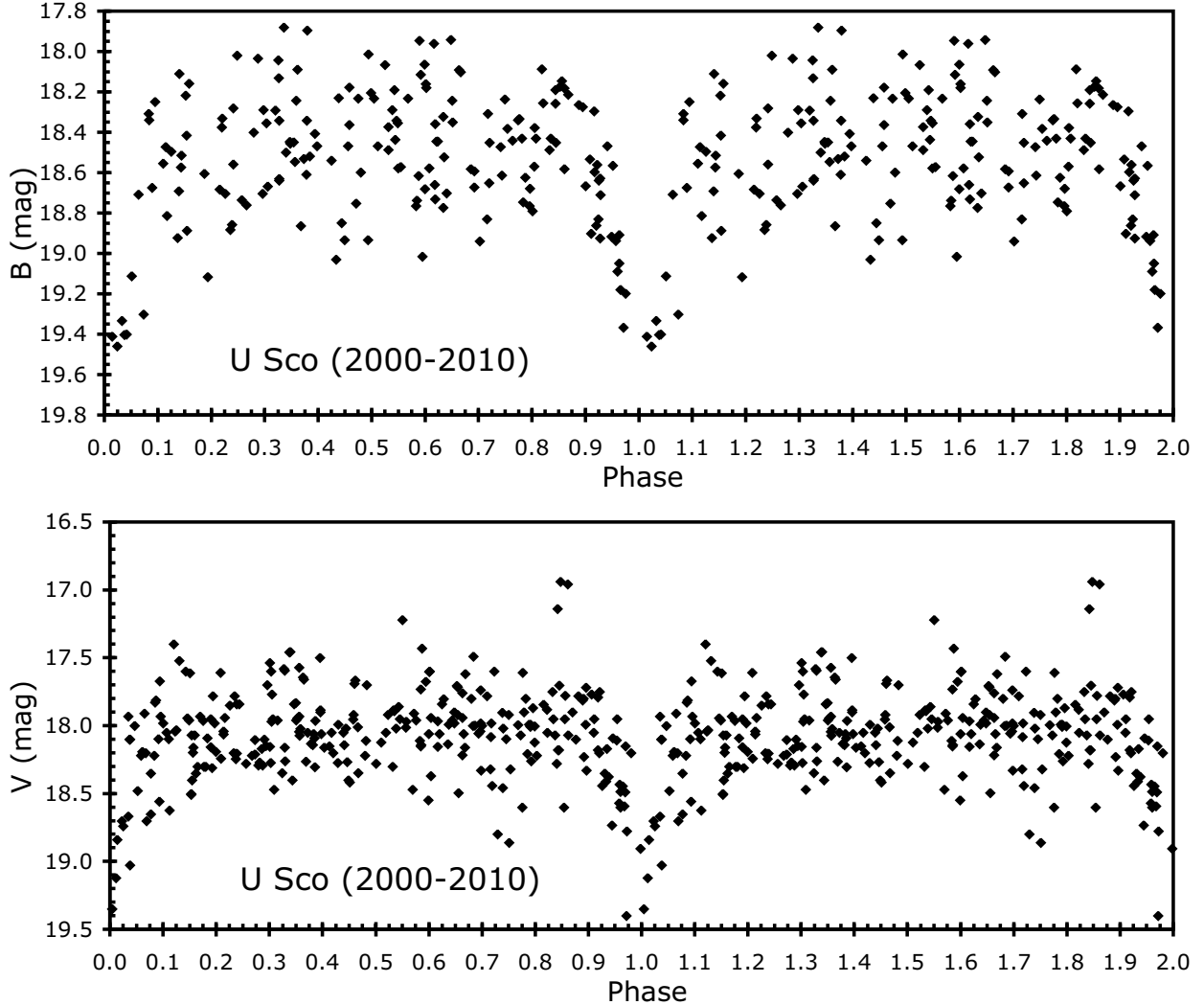


Fig. 3.— U Sco phased light curve in B and V. The two panels show the B and V magnitudes as a function of U Sco’s orbital phase for all observations from 2000 until the 2010 eruption. Each magnitude is double plotted, once for phases 0-1 and a second time with unity added to the phase, so as to ease the visibility of the eclipse. Both light curves show substantial short-term variations superposed on a flat light curve with eclipses. The eclipses look rather ragged, the result of taking one isolated point from many eclipses over which the system is varying up and down. (Time series through individual eclipses show a well-defined classic eclipse shape.) No secondary eclipse is visible in either B or V. Note that the scatter apparent outside of eclipse is much smaller during the eclipse, pointing to the flickering region being eclipsed.